Characterizing the Spatial and Temporal Distribution of Aerosol Optical Thickness Over the Atlantic Basin Utilizing GOES-8 Multispectral Data

Final Report
NASA Grant NAG5-4751

Co – Investigators

Robert Fox
Former Executive Director, SSEC

Elaine M. Prins
NOAA/NESDIS/ORA/ASPT
ph: (608) 263-6607
email: elaine.prins@ssec.wisc.edu
fax: (608) 262-5974

Prepared By

Joleen M. Feltz (UW-Madison CIMSS)
Elaine M. Prins (NOAA/NESDIS/ORA/ASPT)

April 2001

TABLE OF CONTENTS

I. Introduction

In recent years, modeling and analysis efforts have suggested that the direct and indirect radiative effects of both anthropogenic and natural aerosols play a major role in the radiative balance of the earth and are an important factor in climate change calculations. The direct effects of aerosols on radiation and indirect effects on cloud properties are not well understood at this time. In order to improve the characterization of aerosols within climate models it is important to accurately parameterize aerosol forcing mechanisms at the local, regional, and global scales. This includes gaining information on the spatial and temporal distribution of aerosols, transport regimes and mechanisms, aerosol optical thickness, and size distributions. Although there is an expanding global network of ground measurements of aerosol optical thickness and size distribution at specific locations, satellite data must be utilized to characterize the spatial and temporal extent of aerosols and transport regimes on regional and global scales. This study was part of a collaborative effort to characterize aerosol radiative forcing over the Atlantic basin associated with the following three major aerosol components in this region: urban/sulfate, Saharan dust, and biomass burning. In-situ ground measurements obtained by a network of sun photometers during the Smoke Clouds and Radiation Experiment in Brazil (SCAR-B) and the Tropospheric Aerosol Radiative Forcing Observational Experiment (TARFOX) were utilized to develop, calibrate, and validate a Geostationary Operational Environmental Satellite (GOES)-8 aerosol optical thickness (AOT) product. Regional implementation of the GOES-8 AOT product was used to augment point source measurements to gain a better understanding of the spatial and temporal distributions of Atlantic basin aerosols during SCAR-B and TARFOX.

The following report provides a summary of the work performed for grant NAG5-4751. During the past three years our efforts focused on

> **a.)** Geostationary Operational Environmental Satellite (GOES)-8 visible calibration;
> **b.)** implementation of an updated smoke and cloud classification technique, the Merged Automated Cloud/Aerosol Detection Algorithm (MACADA);
> **c.)** development, implementation, and testing of the experimental CIMSS GOES-8 Aerosol Optical Thickness (AOT) algorithm throughout the Atlantic basin with applications over land and water;
> **d.)** application of the CIMSS GOES-8 AOT algorithm in South America and the South Atlantic Ocean for 24 days at the height of the South American fire season during SCAR-B (15 August – 7 September, 1995).
> **e.)** application of the CIMSS GOES-8 AOT algorithm in the eastern portion of North America and the North Atlantic Ocean for 21 days during TARFOX (11 –31 July 1996);
> **f.)** and comparisons of AOTs derived from GOES-8 and sun photometer sites.

We also completed a five-year trend analysis of fires, smoke, and cloud-types in South America under separate funding.

II. GOES-8 Visible Calibration

A major aspect of this study involved addressing the degradation in the GOES-8 visible channels and its impact on GOES derived AOTs using the new CIMSS algorithm. We initially used a visible calibration offset of 5% per year based on calibration studies performed by Dr. M. Weinreb and Dr. N. Rao of NOAA/NESDIS, and Dr. G. Diak of UW-Madison CIMSS. This degradation resulted in GOES-8 derived AOTs that were significantly lower than those derived from the AERONET sun photometer network in South America. Recent work by Dr. K. Knapp and Dr. T. Vonder Haar (CIRA, Colorado State University) have suggested that the GOES-8 visible degradation includes an initial drop of 7.6% and an additional drop of 5.6% each year following the launch. Based on earlier studies by Knapp and Vonder Haar, an initial drop of 10.4% and additional drops of 5.6% per year were used in this study. GOES-8 AOT values derived using these calibration offsets are generally more in line with sun photometer derived AOTs, but the improvement is also highly dependent on the scattering properties assumed for the smoke aerosol and clear-sky background visible reflectance determination.

III. Implementation of the GOES-8 MACADA and ABBA in South America

In an effort to develop a more robust GOES-8 AOT product, the GOES-8 Merged Automated Cloud/Aerosol Detection Algorithm (MACADA) was revised based on real-time applications of the MACADA during the 1999 fire season. The improvements have resulted in better discrimination between clouds, smoke/aerosol, and clear sky throughout the day over both South America and the Atlantic Ocean. This is especially important in determining accurate clear-sky values for AOT retrievals.

Under separate funding, the MACADA was applied to South America and the South Atlantic at 1145, 1445, 1745, and 2045 UTC during the 1995, 1996, 1997, 1998, and 1999 fire seasons (June-October). The GOES-8 Automated Biomass Burning Algorithm (ABBA) was applied to the same time periods. Together these algorithms were used to document diurnal, spatial, and interannual trends in fires, smoke, and clouds. Figure 1 shows the seasonal GOES ABBA fire composites and opaque cloud coverage at 1745 UTC and aerosol/smoke coverage at 1145 UTC for each of the five years. Similar burning patterns are depicted in each year. Peak burning was observed in the Brazilian states of Para, Tocantins, and Maranhao (**A**); Mato Grosso (**B**); Rondonia (**C**); and in Amazonas/Acre (**D**) where a new road is being built to the Pacific Ocean. Fires were also detected in Bolivia, Paraguay, and northern Argentina. Each year the GOES-8 MACADA results show large regions of South America covered with smoke over 20% of the time with noticeable interannual differences. The aerosol/smoke composites closely reflect interannual differences in fire activity. Throughout the arc of deforestation opaque cloud coverage is typically on the order of 10 to 20%.

Although the same basic patterns are observed each year, differences are noted in fire activity, smoke coverage and opaque cloud coverage. The difference composites in figure 2 compare the 1995 benchmark year with subsequent fire seasons. In the fire difference plots, the regions shaded in orange-red-magenta represent areas where fire activity was greater in

Five-year Summary of Fires, Opaque Cloud, and Aerosol/Smoke Coverage
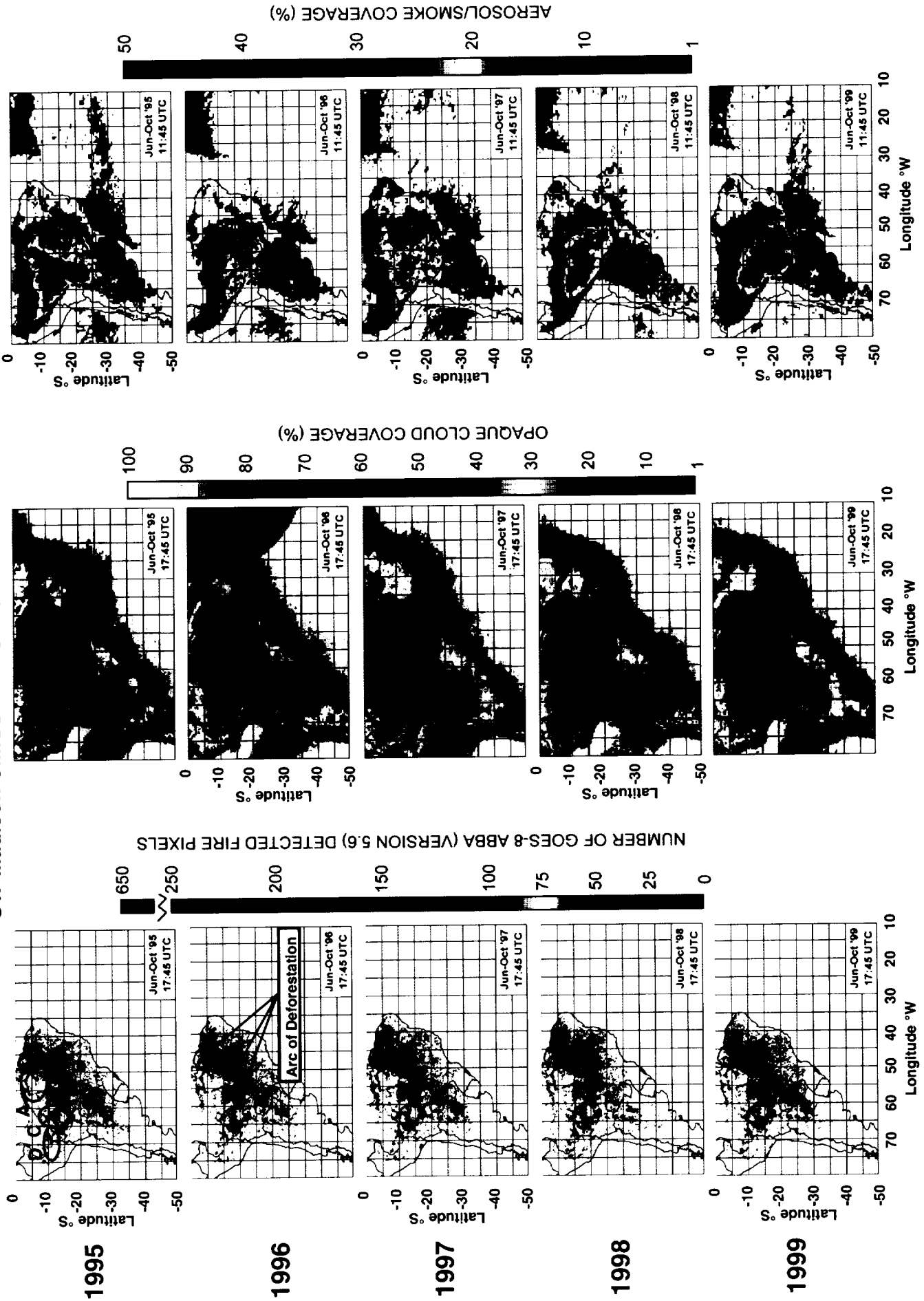### UW-Madison CIMSS   NOAA/NESDIS/ORA/ASPT

Figure 1

-3-

Interannual Differences in Fires, Opaque Clouds, and Aerosol/Smoke:
Each Year Compared to 1995 Benchmark Year
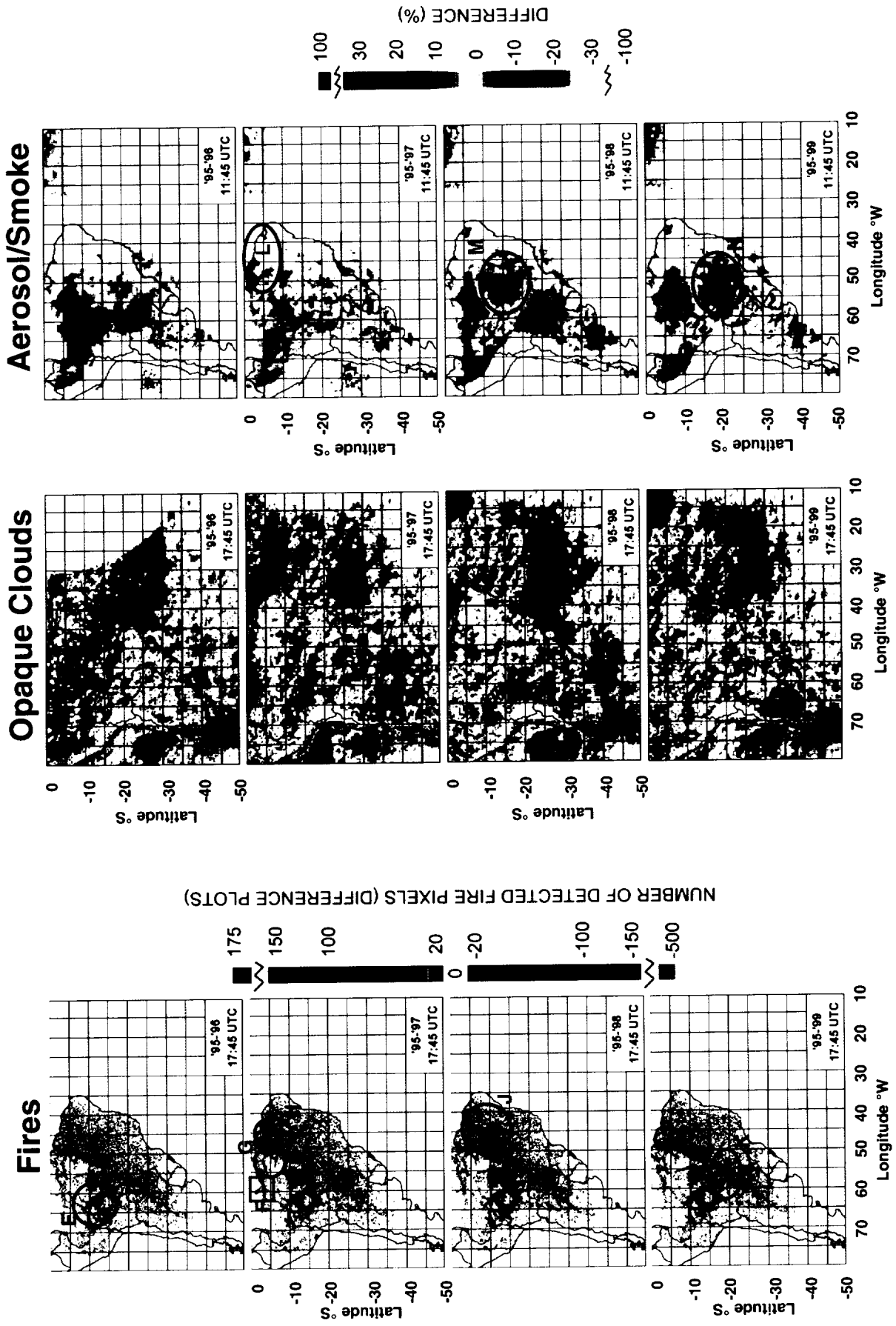### UW-Madison CIMSS   NOAA/NESDIS/ORA/ASPT

Figure 2

-4-

1995; blue-green regions represent areas where fire activity was greater in the respective year. A quick overview of the five years shows that 1995 was the peak year especially in Rondonia (E). In 1997 there was increased activity north of Manaus (location F) and in central and northeastern Brazil (G, H, I) due to drought conditions associated with El Nino. In 1998 the ABBA detected elevated burning in eastern Brazil (J). In 1999 enhanced fire activity was observed in southwestern Brazil, Paraguay, and Bolivia (K) where wildfires raged out of control. Interannual differences in opaque cloud cover were less than 2% on average throughout the fire study area. The aerosol/smoke difference composites closely reflect the differences in burning with maximum smoke coverage in 1995. In 1997 there was a slight increase in smoke coverage in northeastern Brazil (L) associated with increased burning in this region. In 1998 greater smoke coverage was observed in southeastern Brazil (M) located downwind of the increased fire activity. In 1999 increased fire activity in Bolivia and southwestern Brazil resulted in higher smoke coverage over southern Brazil (N).

During the upcoming year we will use this 5-year cloud type and aerosol data base to investigate the possible impacts of smoke on cumulus cloud formation and other smoke/cloud interactions. This work will be supported under separate funding.

IV. Development of the Experimental CIMSS GOES-8 AOT Algorithm: Applications Over Land and Water:

A. Generation of AOT Lookup Tables

Case studies from the TARFOX field program indicated that a different set of look-up tables were required to produce an improved GOES-8 AOT product. The GOES-8 AOT algorithm developed at CIMSS includes new AOT look-up tables created in collaboration with B. Baum (NASA–LaRC), S. Kinne (NASA–GSFC), and S. Christopher (University of Alabama – Huntsville). The look-up tables were generated using a model developed by Tsay and Stephens. This model provides Mie solutions of scattering properties for aerosol distributions that may consist of any user-specified combination of dust, soluble and nonsoluble particles, water droplets, soot, and sulfuric acid. Further, the aerosol scattering properties of these assumed distributions are a function of the atmospheric humidity. In a humid environment, some of the particles may become coated with water, thereby changing the bulk scattering properties of the aerosol. The method produces bulk scattering quantities such as scattering phase function, extinction and backscatter coefficients, and single scatter albedo. B. Baum used the bulk quantities to generate look-up tables for a range of single scattering albedos while keeping the size distribution constant. The range of single scattering albedos used for applications during SCAR-B was between 0.77 and 0.95. Different single scattering albedos were used for the study of aerosol in the north Atlantic basin; the values were 0.92, 0.96 and 0.9788.

A discrete ordinates radiative transfer model was employed for the development of the GOES-8 AOT look-up tables. The tables provide the relationship of AOT to observed visible reflectance above clear-sky background reflectance for AOT values ranging from 0 to 3 in 0.25 increments and then in 0.5 increments for AOT values from 3 to 10. The table provides a

lookup for solar zenith angles from 0-84° in 6° increments, vertical zenith angles from 0-84° in 6° increments, and azimuth angles from 0-180° in 10° increments. Results vary according to chosen values of the single scattering albedo and the viewing geometry. However, the reflectance of smoke tends towards a constant value near an optical thickness of 2, meaning that there is little ability to infer accurate AOT from the GOES visible channel for relatively thick smoke, often observed over South America. This was not an issue for the urban aerosol and dust observed during TARFOX, since most of the derived AOT values were well below 1.0.

B.   CIMSS GOES-8 AOT Processing Methodology

Figures 3, 4, and 5 demonstrate the process used to derive GOES AOT for three time periods (1145, 1445, 1745 UTC) at the peak of the fire season in South America on 26 August 1995. Figures 3a, 4a, and 5a show smoke palls as observed in GOES visible imagery. GOES multispectral imagery are processed with the MACADA to automatically discriminate between smoke, clouds, and clear sky. Initially the MACADA uses a textural scheme and some spectral tests based on the Automated Smoke Aerosol Detection Algorithm (ASADA) to discriminate between cloud types, smoke, and clear-sky. Figures 3b, 4b, and 5b show the results of this initial step at 1145, 1445, and 1745 UTC, respectively. Once this is complete, additional spectral tests are used to further discriminate between clouds, smoke, and clear sky. Figures 3c, 4c, and 5c show the final smoke and clear-sky image as determined by the MACADA. This image is used to indicate clear sky in the corresponding visible image.

In the process of creating a background clear-sky map (figures 3d, 4d, and 5d) for South America, all clear-sky raw visible values in a 9x9 box (4 km resolution) are averaged over a period of 14 days; the lowest clear-sky average of the 14 days for each 9x9 box is selected. The process was similar for the TARFOX study, except all the available days (11 – 31 July, 1996) were used to create a clear-sky map for each time period. Depending on the time period, the number of days which comprised the clear-sky background during TARFOX ranged from 18-20 days. A clear-sky map is determined using a solar zenith angle corrected albedo calculated from the clear-sky raw visible values average minus one standard deviation in each of the 9x9 boxes. If no clear-sky background values are available, a 14-day ecosystem based clear-sky map is used (figures 3e, 4e, and 5e). This map is based on the Olson ecosystem classification where all clear-sky reflectances are grouped by ecosystem type and weighted according to sun angle. An ecosystem albedo minus one standard deviation is applied to every pixel within that ecosystem. Excluding albedos in regions where the reflected sun angle was less than or equal to 27.5° eliminated biases from solar reflectance. The reflected sun angle (θ) was calculated using the following equation where θ_0 is the solar zenith angle, θ is the satellite zenith angle, and ψ is the relative azimuth angle:

$$\cos\theta = \sin\theta\sin\theta_0\cos\psi + \cos\theta\cos\theta_0$$

A solar zenith angle cut-off of 82.5° was used to avoid areas of darkness, and satellite zenith angles greater than 60.0° were not considered to eliminate ecosystem albedo biases introduced when the western edge of the African continent is included. The reflected sun angle and the

GOES-8 Experimental AOT Analysis: 26-August-1995 at 1145 UTC

UW-Madison/SSEC/CIMSS
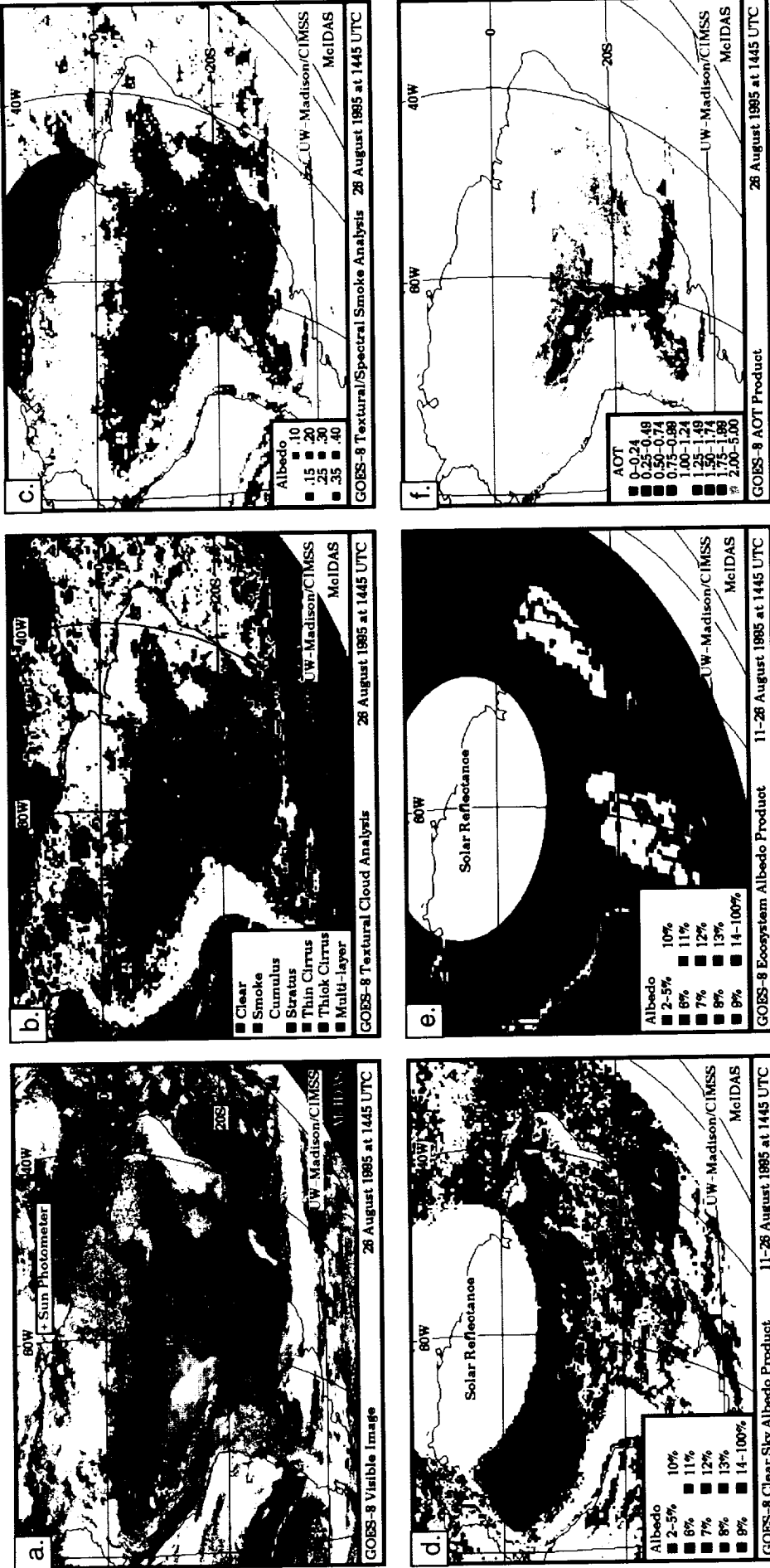
NOAA/NESDIS ORA/ASPT
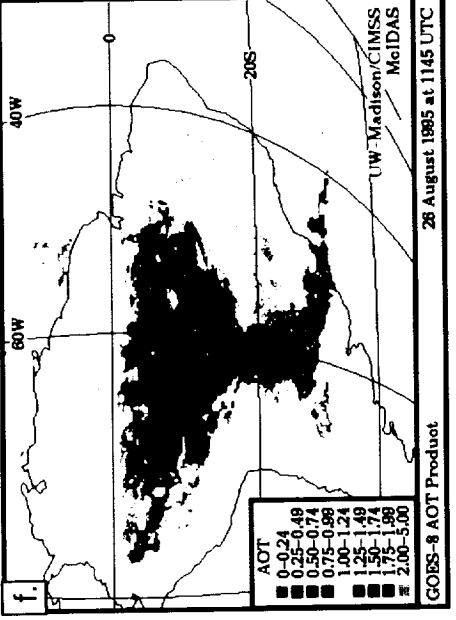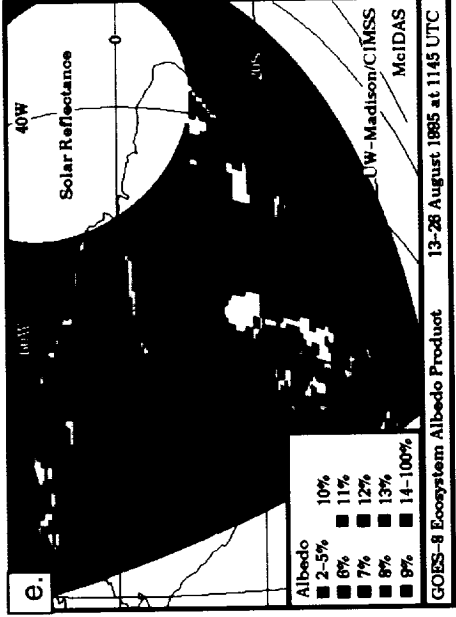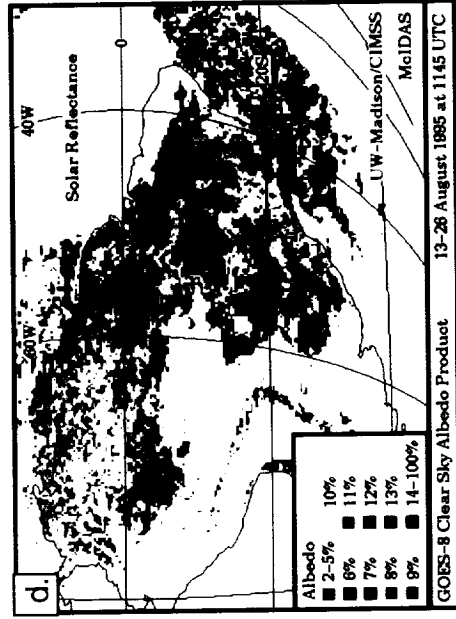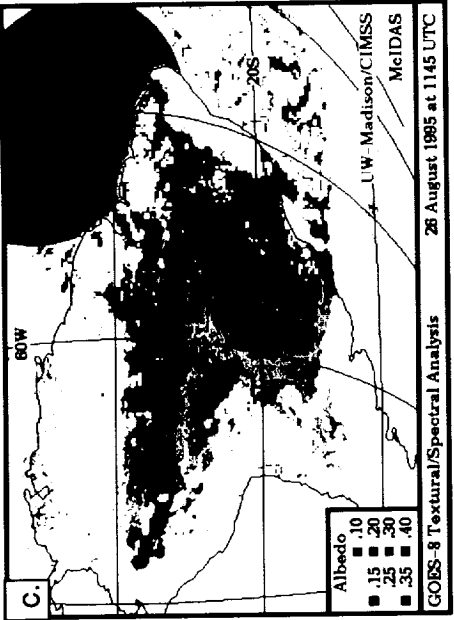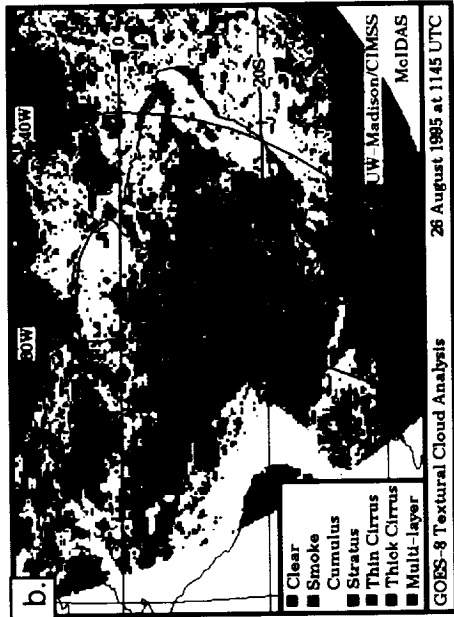
Panel a shows smoke as observed in GOES-8 visible imagery at 1145 UTC on 26 August 1995. The GOES-8 MACADA is applied to multi-spectral GOES imagery to automatically distinguish between clear-sky, cloud type, and smoke using both textural and spectral techniques (panels b and c). The MACADA textural/spectral analysis is then used to create a 14-day clear-sky background reflectance map shown as solar zenith weighted albedo (panel d). The AOT product (panel f) is determined by calculating the difference between the observed and clear-sky reflectance and relating this to AOT utilizing a look-up table. If no clear-sky reflectance is available for a given location, an ecosystem based reflectance map (panel e) is used.

Figure 3

-7-

GOES-8 Experimental AOT Analysis: 26-August-1995 at 1445 UTC

UW–Madison/SSEC/CIMSS

NOAA/NESDIS ORA/ASPT
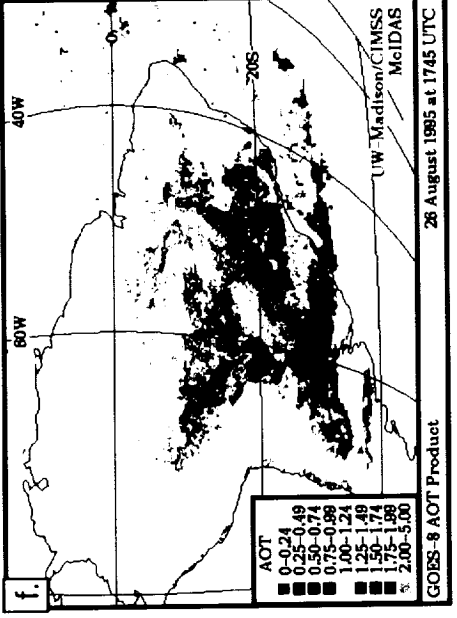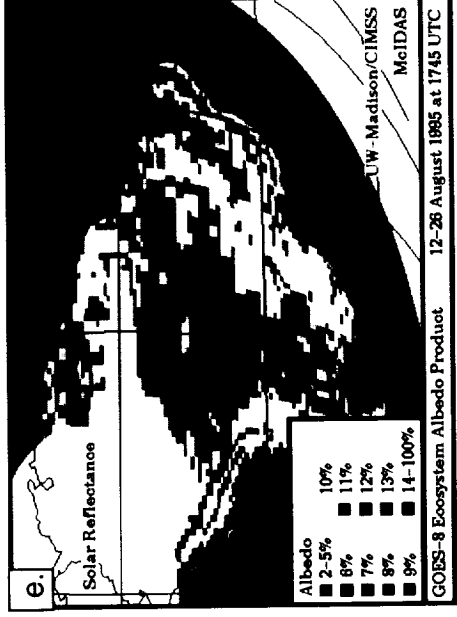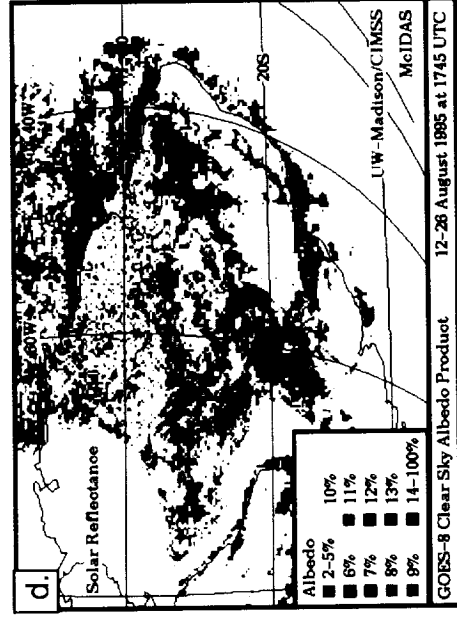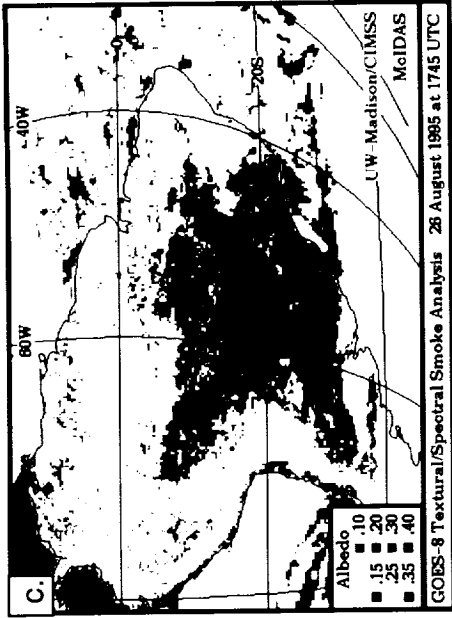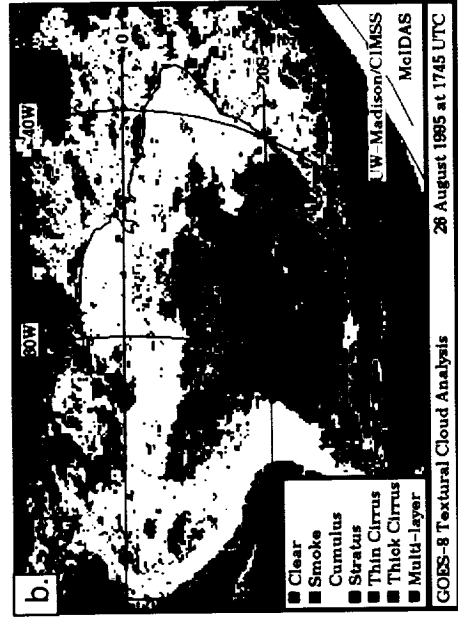

Panel a shows smoke as observed in GOES-8 visible imagery at 1445 UTC on 26 August 1995. The GOES-8 MACADA is applied to multi-spectral GOES imagery to automatically distinguish between clear-sky, cloud type, and smoke using both textural and spectral techniques (panels b and c). The MACADA textural/spectral analysis is then used to create a 14-day clear-sky background reflectance map shown as solar zenith weighted albedo (panel d). The AOT product (panel f) is determined by calculating the difference between the observed and clear-sky reflectance and relating this to AOT utilizing a look-up table. If no clear-sky reflectance is available for a given location, an ecosystem based reflectance map (panel e) is used.

Figure 4

-8-

GOES-8 Experimental AOT Analysis: 26-August-1995 at 1745 UTC

UW–Madison/SSEC/CIMSS   NOAA/NESDIS ORA/ASPT

Panel a shows smoke as observed in GOES-8 visible imagery at 1745 UTC on 26 August 1995. The GOES-8 MACADA is applied to multi-spectral GOES imagery to automatically distinguish between clear-sky, cloud type, and smoke using both textural and spectral techniques (panels b and c). The MACADA textural/spectral analysis is then used to create a 14-day clear-sky background reflectance map shown as solar zenith weighted albedo (panel d). The AOT product (panel f) is determined by calculating the difference between the observed and clear-sky reflectance and relating this to AOT utilizing a look-up table. If no clear-sky reflectance is available for a given location, an ecosystem based reflectance map (panel e) is used.

Figure 5

solar zenith angle cut-offs remained the same for TARFOX; but, the satellite zenith angle cut-off was increased to 65° since there were no albedo biases due to continents on the edge of the study domain.

The GOES-8 AOT retrieval is made by initially comparing the measured GOES-8 visible reflectance with the calculated clear-sky background visible reflectance. This difference is converted to AOT by using look-up tables which list visible reflectances above background as a function of AOT and satellite viewing geometry. Figures 3f, 4f, and 5f show the Experimental CIMSS GOES-8 AOT product using a single scattering albedo of 0.90. All three time periods show elevated AOTs in southwest Brazil (Rondonia) and Bolivia. At 1445 UTC the CIMSS GOES-8 AOT algorithm identified a region southwest of the sun photometer sites in Rondonia where the AOTs were greater than 2 and occasionally exceeded the maximum plotted AOT of 5. As stated earlier, it is difficult to accurately determine GOES-8 AOTs for relatively thick smoke (i.e. AOTs greater than 2) using our current methodology.

V. Application of the CIMSS GOES-8 AOT During SCAR-B: Analysis of Biomass Burning Aerosols

A. Comparisons of Clear-Sky Maps for South America and the South Atlantic

Comparison of the clear-sky maps based on local 14-day GOES visible observations and the ecosystem based reflectance maps show albedo differences typically on the order of 0-2% as seen in figure 6. Higher differences are found at 1145 UTC where low sun angles and smoke make it difficult to retrieve representative visible albedos in Northwestern Amazonia. Furthermore, highly reflective surfaces and some cloud contamination in southeastern Amazonia introduce larger differences at 1145 and 1445 UTC.

B. CIMSS GOES-8 Derived AOT Results During SCAR-B: 15 August – 7 September 1995

After the third year report was completed, it was determined that the relative azimuth input to the AOT look-up table was 180° out of phase. The entire SCAR-B dataset was reprocessed using the corrected azimuth angles and the new results are reported here.

The revised CIMSS GOES-8 AOT algorithm was applied to 24 days of data obtained during the SCAR-B study period (15 August – 7 September 1995) at 1145, 1445, and 1745 UTC using a variety of single scattering albedos. The reprocessed GOES-8 AOT product showed the largest change at 1145 UTC, in part due to the strong forward scattering at this time of the day. GOES-8 derived AOT values were much lower at 1145 UTC than originally reported. Figure 7 shows the GOES-8 derived AOT product using single scattering albedos of 0.83, 0.90 and 0.95 for 26 August 1995 at 1145, 1445, and 1745 UTC, respectively. The gradient in AOT at 1145 UTC is smaller than shown in the third year report. The other time periods show less change. Although the derived AOTs using each of the single scattering albedos all show elevated values along the Brazil/Bolivia border, the magnitude is strongly dependent on the single scattering albedo. Table 1 shows how the GOES derived AOT at
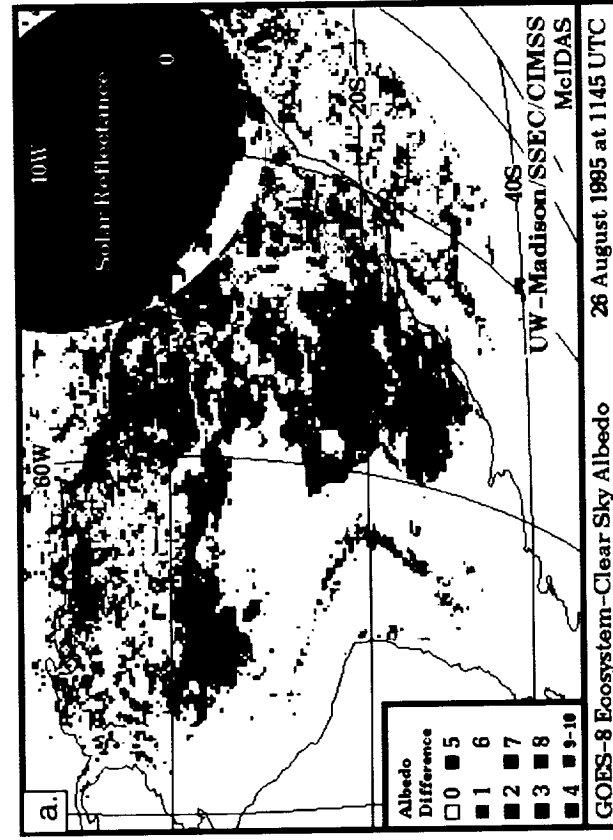
Difference between Ecosystem and Clear Sky Reflectance/Albedo Product
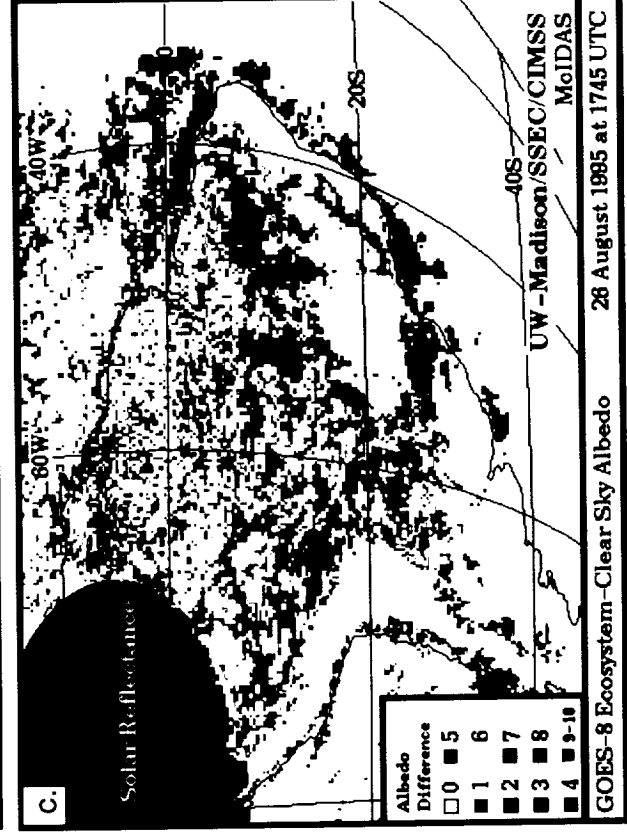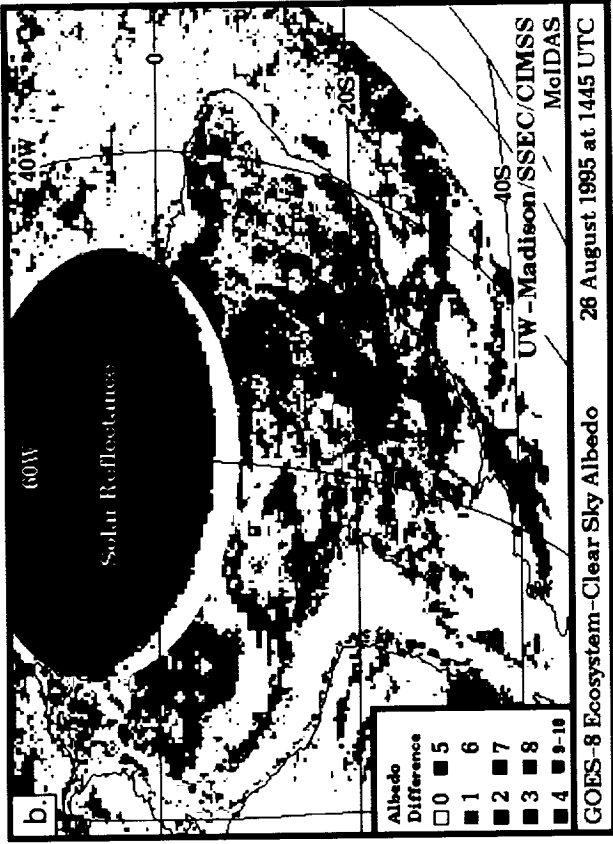
Comparison of the clear-sky maps based on local 14-day observed clear-sky values versus the ecosystem based clear-sky maps generally show albedo differences on the order of 0-2%. Higher differences are found at 1145 UTC where low sun angles and smoke make it difficult to retrieve clear-sky values in northwestern Amazonia and in southeastern Brazil due to highly reflective surfaces and some cloud contamination along the persistent frontal boundary.

Figure 6

Comparison of
GOES-8
Derived AOT
Using
Single Scattering
Albedos of
.83, .90, and .95
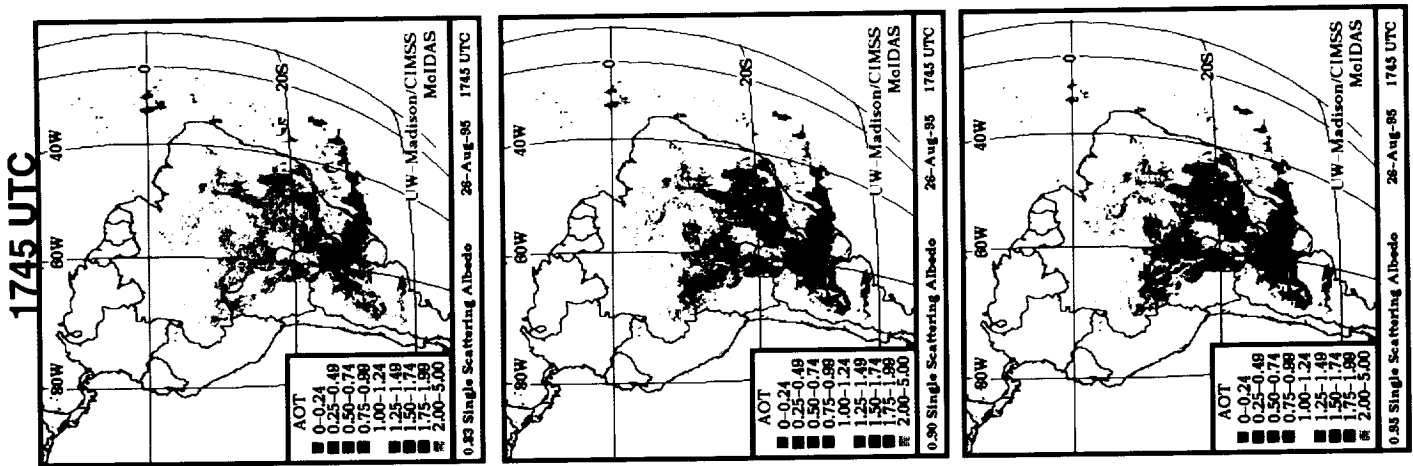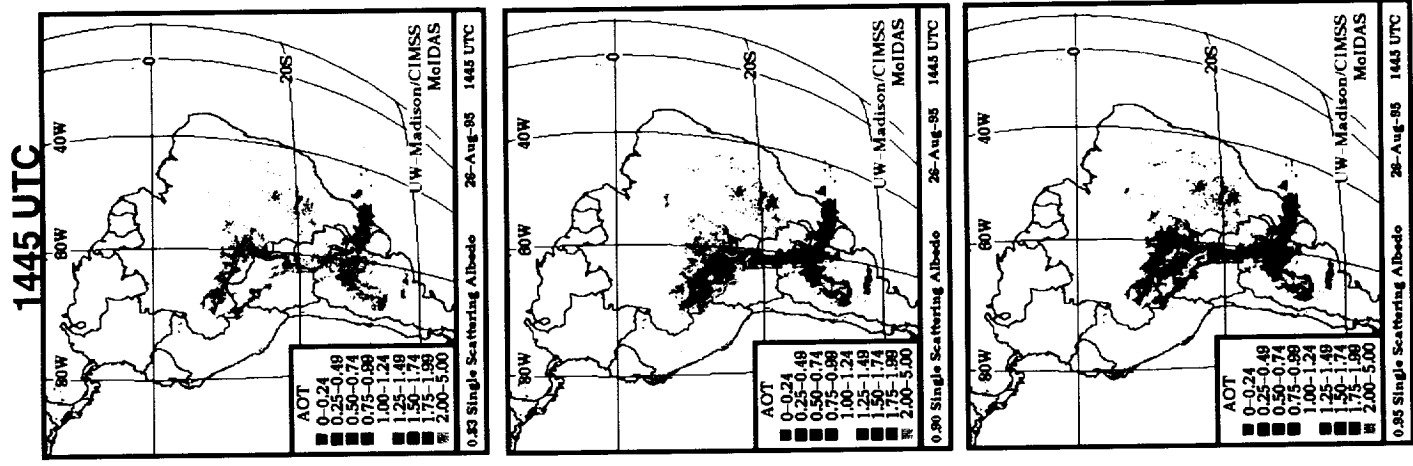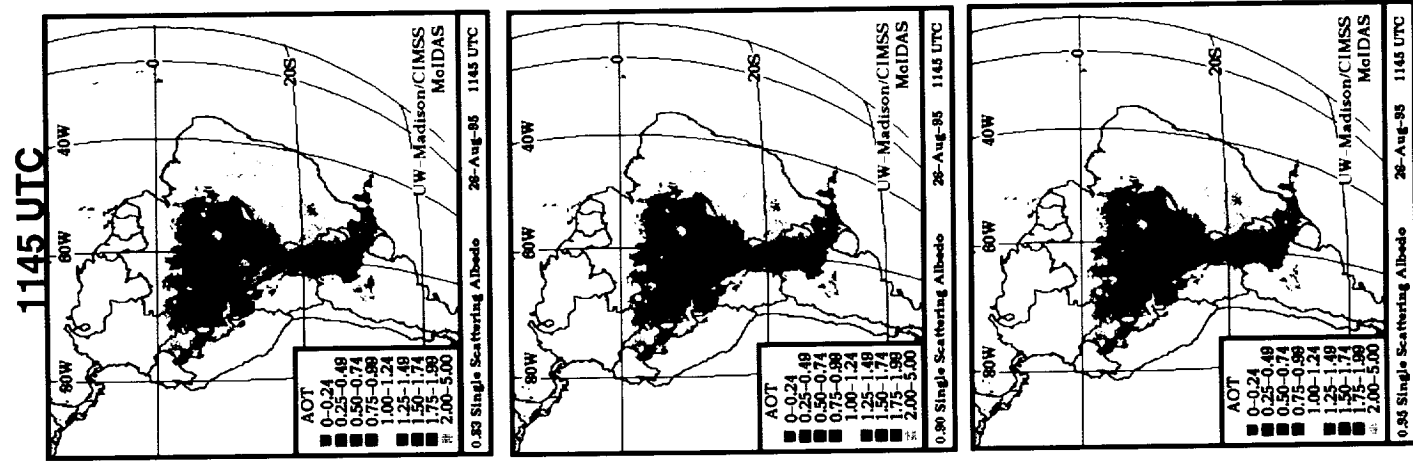
Date: 26-Aug-95
at
1145, 1445, 1745 UTC

-12-

Figure 7

9:59:50 °S and 65:17:26 °W varies at 1145, 1445, and 1745 UTC on 26 August 1995 according to the input single scattering albedo. Figure 8 shows the average GOES-8 AOT product for the time period 15 August – 7 September 1995. Table 2 shows a comparison of 24-day averaged GOES-8 derived AOTs for the same location using different single scattering albedos. Similar variability is observed.

Table 1: GOES-8 Derived AOT Product at 9:59:50 °S, 65:17:26 °W on 26 August 1995.

	Time		
Single Scattering Albedo	**1145 UTC**	**1445 UTC**	**1745 UTC**
0.83	0.6	2.2	1.2
0.90	0.4	1.1	0.7
0.95	0.3	0.9	0.6

Table 2: GOES-8 Derived Average AOT Product at 9:59:50 °S, 65:17:26 °W for the time period 15 August – 7 September 1995.

	Time		
Single Scattering Albedo	**1145 UTC**	**1445 UTC**	**1745 UTC**
0.83	0.5	3.0	2.3
0.90	0.4	1.3	1.0
0.95	0.3	0.9	0.8

Independent studies, field measurements, and comparisons with sun photometer derived AOTs have indicated that a single scattering albedo of 0.90 is the most appropriate for smoke aerosol in South America. The 24-day average GOES-8 AOT product (figure 8) based on a single scattering albedo of 0.90 shows elevated values of AOT associated with smoke that builds up along the eastern edge of the Andes mountain range. Generally, the circulation pattern transports the smoke counter-clockwise from Amazonia to the Andes Mountains. The smoke then gets trapped along the eastern slopes of the Andes Mountains and travels southward before traveling eastward over the Atlantic Ocean near 35°S. GOES-8 derived AOT values at 1445 UTC are elevated throughout the arc of deforestation and northern Bolivia and in Paraguay. At 1745 UTC most of the higher AOT values are confined to the western portion of the Amazon basin and Northern Bolivia. The highest GOES-8 AOT values were recorded in northeastern Bolivia; GOES-8 derived AOT values for this region were on average greater than 1.5. It is important to note that in August 1995, the sun photometer network did not include an operational monitoring site in this region during the peak of the fire season.

Comparison of
GOES-8
Derived AOT
Using
Single Scattering
Albedos of
.83, .90, and .95
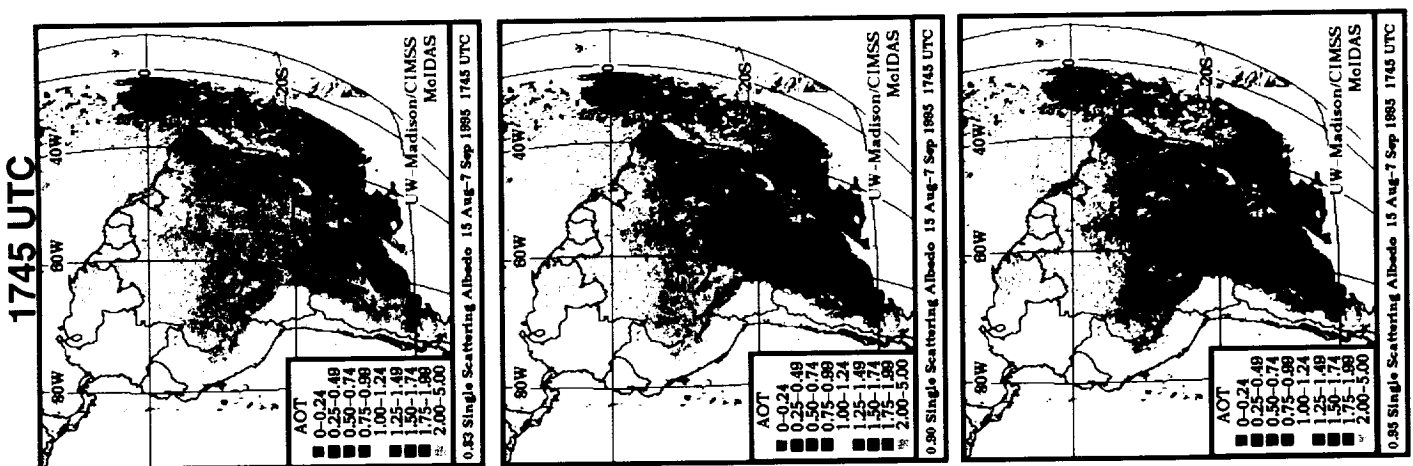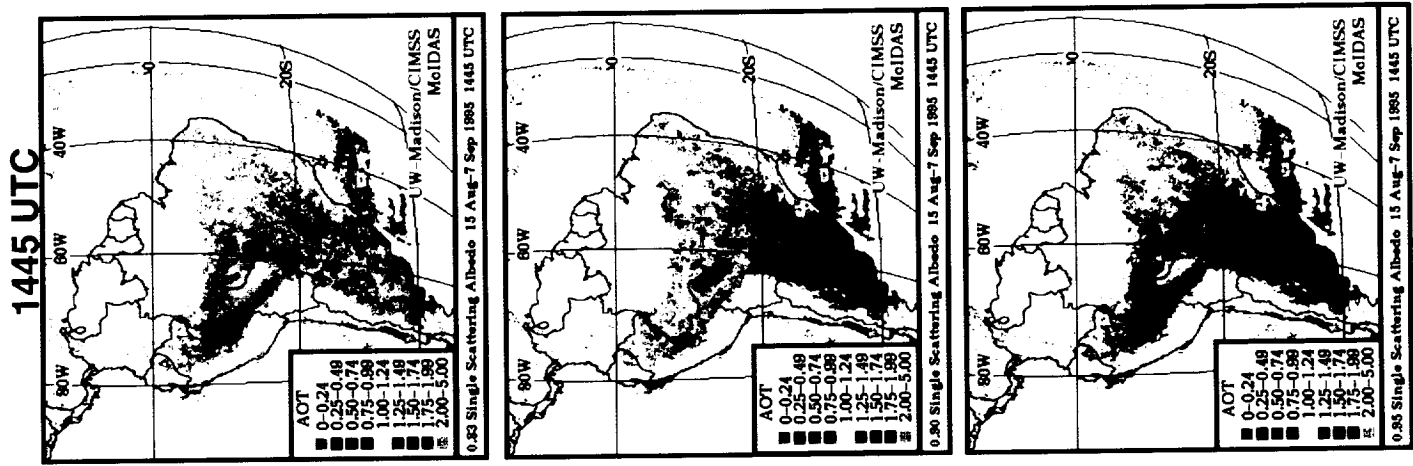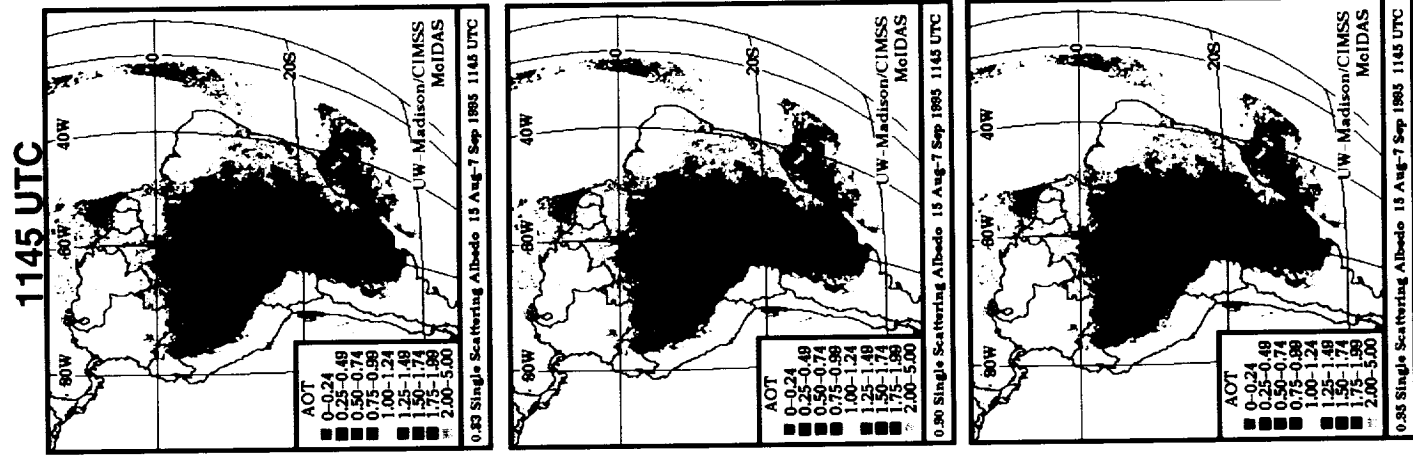
Study Period:

8/15/95 - 9/7/95
at
1145, 1445, 1745 UTC

-14-

Figure 8

C. Comparisons of CIMSS GOES-8 and Sun Photometer Derived AOTs

GOES-8 derived AOTs were calculated using models based on a range of single scattering albedos. The GOES-8 derived AOTs were then compared to the sun photometer derived AOTs at various locations in South America by selecting the sun photometer values within ten minutes of the satellite viewing time. Statistics were calculated for both the AOT retrieved at the latitude and longitude of the sun photometer site and the best match within three pixels in any direction from the sun photometer site, to account for navigation offsets. Figure 9 shows the correlation between the experimental GOES-8 derived AOT and sun photometer derived AOT using various single scattering albedos. The solid line depicts a perfect one-to-one correlation between the GOES and sun photometer derived AOT value; the dashed lines indicates the actual best-fit linear regression between the two. The correlation of the best match pixels is good, with correlation coefficients varying from 0.82 to 0.93, depending on the time of day and model used. The correlation coefficients were highest for GOES-8 AOTs based on a single scattering albedo of 0.90. Much of the scatter occurs when the AOT exceeds a value of 1.5.

The impact of the reprocessing was most obvious at 1145 UTC. At 1145 UTC the GOES derived AOTs consistently revealed a substantial low bias when compared with the sun photometer derived AOTs, but the statistical correlation of the linear regression improved over the earlier results. The strong linear correlation and consistent low bias seem to indicate that there may be an offset based on viewing geometry. Values changed less at 1445 UTC since it is near solar noon, and there is little forward or backscatter. A slight change was observed in the 1745 UTC correlation results and the AOT values increased minimally. At both 1445 and 1745 a slight high bias was observed for GOES derived AOT values (0.90 single scattering albedo) less than 1.0 and a low bias was observed for values greater than 1.0.

VI. Applications of the CIMSS GOES-8 AOT During TARFOX: Analysis of Urban/Industrial and Dust Aerosols

A. Comparisons of Clear-Sky Maps for North America and the North Atlantic

Comparisons of the clear-sky maps based on local 18-20 day GOES visible observations and the ecosystem based reflectance maps for 21 July 1996 are presented as difference composites in figure 10 for every hour from 1145 to 1845 UTC. These differences are representative of the other days in TARFOX since the same days were used to create the clear-sky maps for the entire period. The only day to day differences would be due to slowly varying solar zenith angle or slight navigation changes. Differences between the clear-sky background and the ecosystem background are 0-2% over water and the variation over land is generally within the same range. Differences over the Great Lakes region, Florida and the Bahamas do exceed these limits during the early morning hours (1145 – 1245 UTC). An artificially high background clear-sky value will produce an AOT which is too low. When the solar zenith angle decreases, the differences in these regions are minimized providing a large portion of the day when the AOT can be retrieved with confidence.

GOES-8 Derived AOTs Compared with Sun Photometer Derived AOTs for SCAR-B Using Single Scattering Albedos of 0.83, 0.90, and 0.95
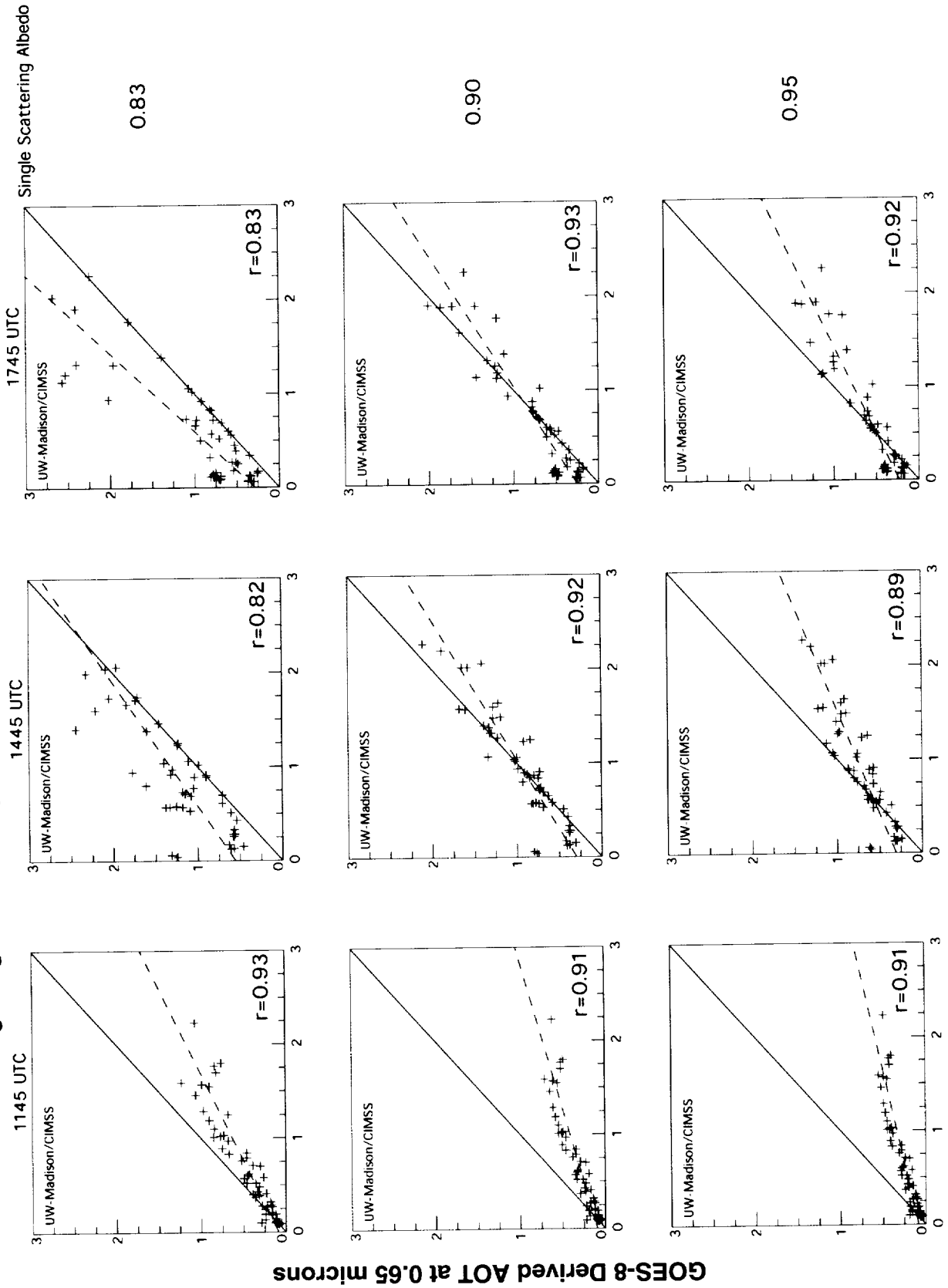
Figure 9

Difference between Ecosystem and Clear Sky Reflectance/Albedo Product

UW–Madison/SSEC/CIMSS   NOAA/NESDIS ORA/ASPT
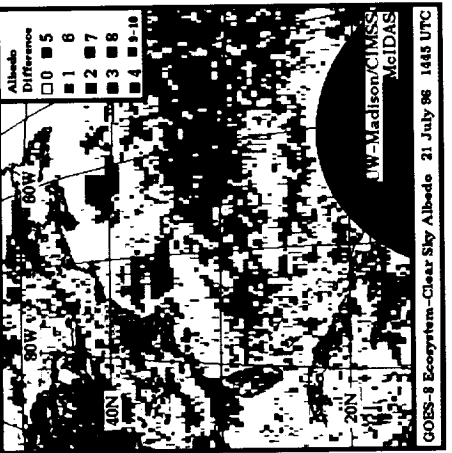
Figure 10

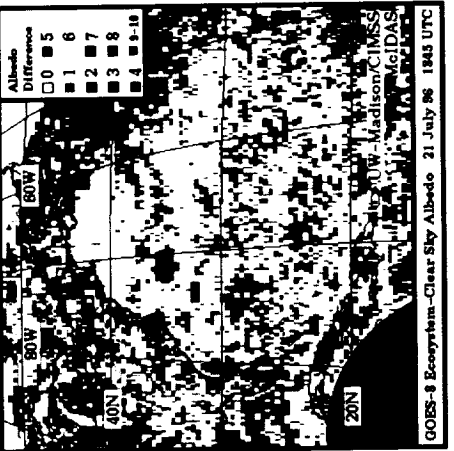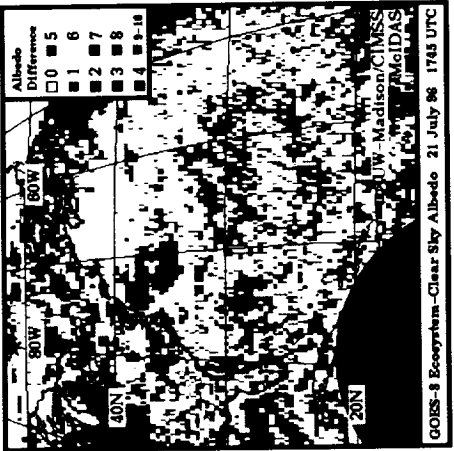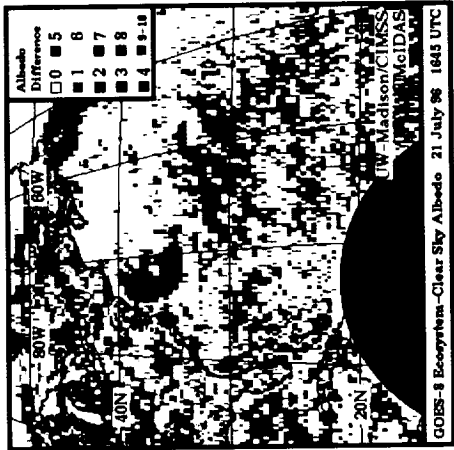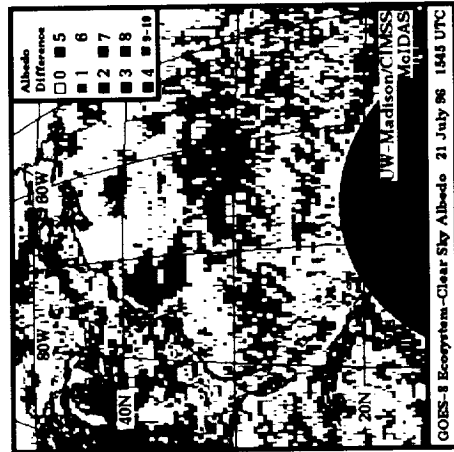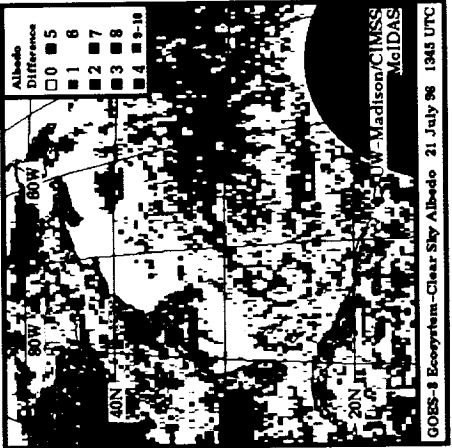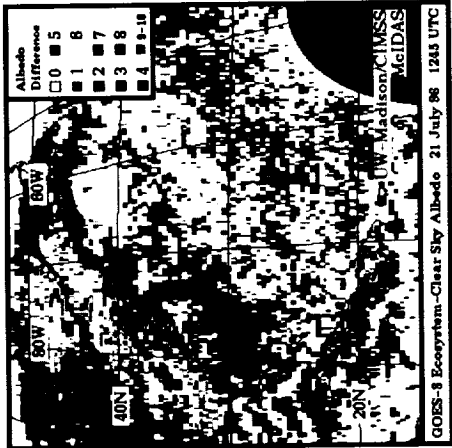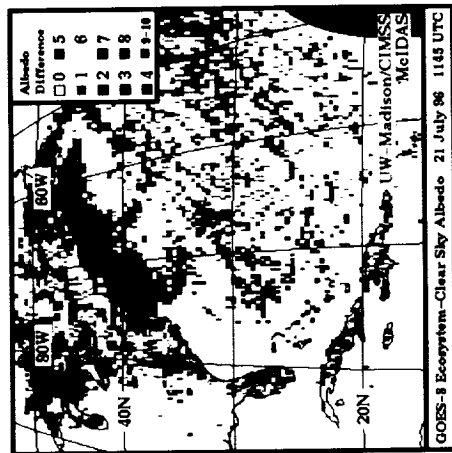**B.   CIMSS GOES-8 Derived AOT Results During TARFOX: 11 – 31 July 1996**

The CIMSS GOES AOT was applied to 21 days of data obtained during the TARFOX field program every hour from 1145 to 1845 UTC. Single scattering albedos of 0.92, 0.96 and 0.9788 were used for this study. These single scattering albedos are representative of maritime conditions including urban pollutants, dust, and sea salt. Figures 11 and 12 provide an example of the hourly CIMSS GOES AOT product from 1145 to 1845 UTC on 21 July 1996 for all three single scattering albedos. Early morning GOES-8 derived AOTs on land and off the East Coast of the U.S. are low. There is an area at 1145 UTC between 20-25°N and 55°W where larger AOT values between 0.20 and 0.30 are observed. The feature persists throughout the day and wind streamline analyses from previous days indicate the dominant upper level flow in that region was conducive for dust transport off the African coast. Near the Florida coast and northward, the flow is from the West off of the continental United States. An increase in AOT along the entire eastern coast of Florida begins to develop near 1345 UTC and persists through 1845 UTC. Increasing values of AOT are observed over land by 1345 UTC, at 9:45 AM in the morning on the East Coast.

Figures 13 and 14 show hourly composites of the average AOT over the entire 21-day period from 11 – 31 July 1996. In all of the panels, there is a general north to south increase in AOT over the Atlantic basin with higher values along the East Coast urban corridor and over the Atlantic Ocean south of 30°N. In the first two panels (1145 UTC and 1245 UTC) the AOT on land tends to be lower than over the ocean. Low AOTs are also observed over the Great Lakes region at 1145 UTC, and are likely due to the artificially high Great Lakes background clear-sky values retrieved for this time period. There is a rapid increase in AOT at 1345 UTC over land; larger AOT values are associated with the major east coast cities and are also observed downwind of the urban centers. There is a persistent elevation of AOT over the ocean within 2° longitude of the coast as compared to further east over the Atlantic Ocean.

**C.   Comparisons of CIMSS GOES-8 and Sun Photometer Derived AOTs**

Diurnal GOES-8 derived AOTs were compared to the sun-photometer derived AOTs over land and water during TARFOX. Figure 15 shows the correlation between the experimental GOES-8 derived AOT and sun photometer derived AOT values. In addition to the sun photometers located on land, Alexander Smirnov provided AOTs derived from sun photometers on board two ships, the "Zenith" and "Meridian." Only the "Meridian" provided AOT values that coincided in time and space with GOES-8 derived AOT values. In figure 15, comparisons over land are indicated by a "plus" sign while comparisons over water are indicated by a triangle. Unlike the GOES-8 derived AOTs during the fire season in South America, the AOT values for the TARFOX comparison study do not exceed 0.8. Linear correlations are good from 1445–1845 UTC with the early morning (1145–1345 UTC) GOES-8 derived AOT values showing a substantial bias toward lower AOTs. AOT calculations using the 0.9788 single scattering albedo were slightly better for most time periods. The model used to generate the AOT look-up table associated with this single scattering albedo was constructed for the maritime environment with soluble particles and salt being the dominant aerosol types. Correlations without ship data (r) range from 0.77–0.97;
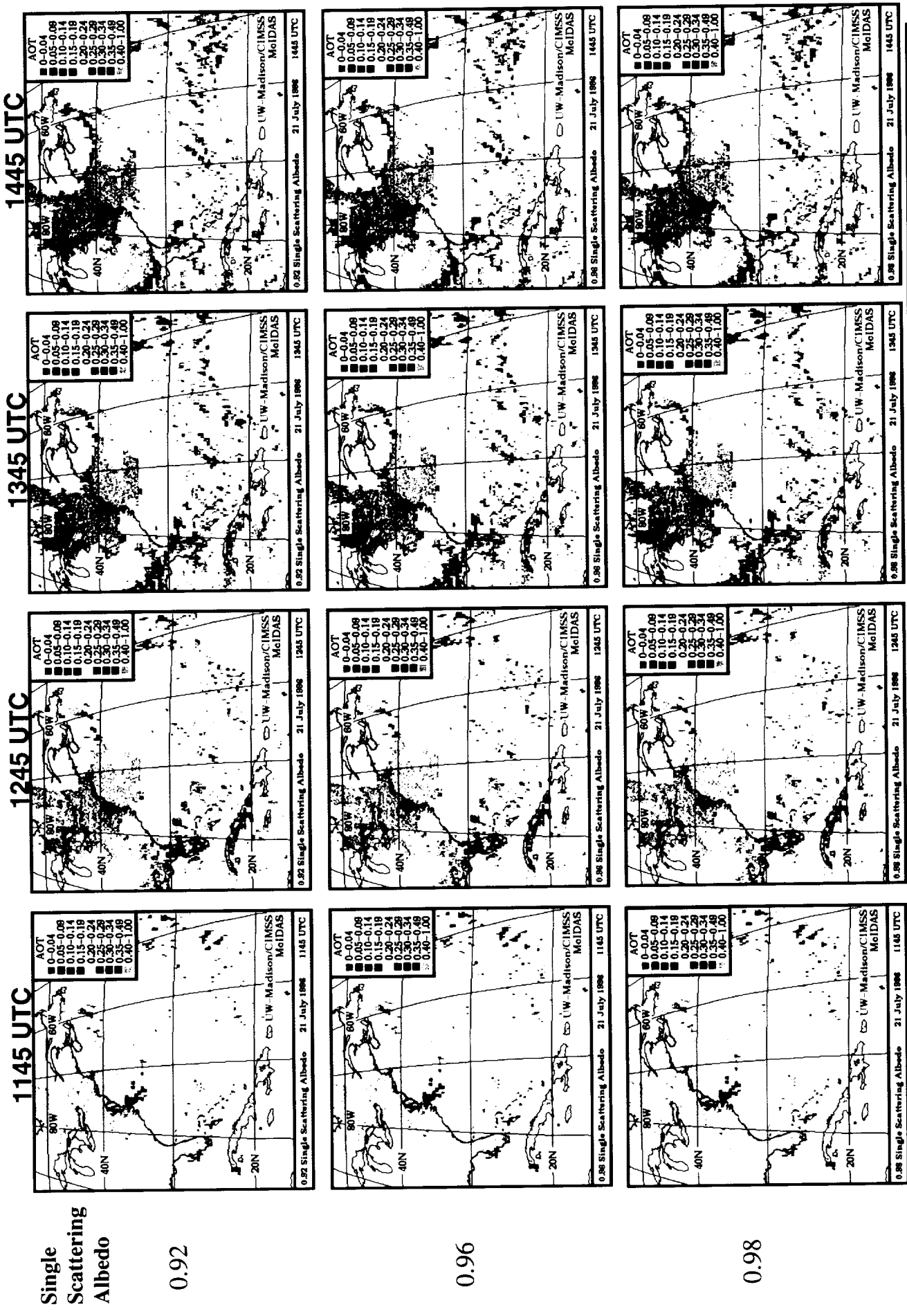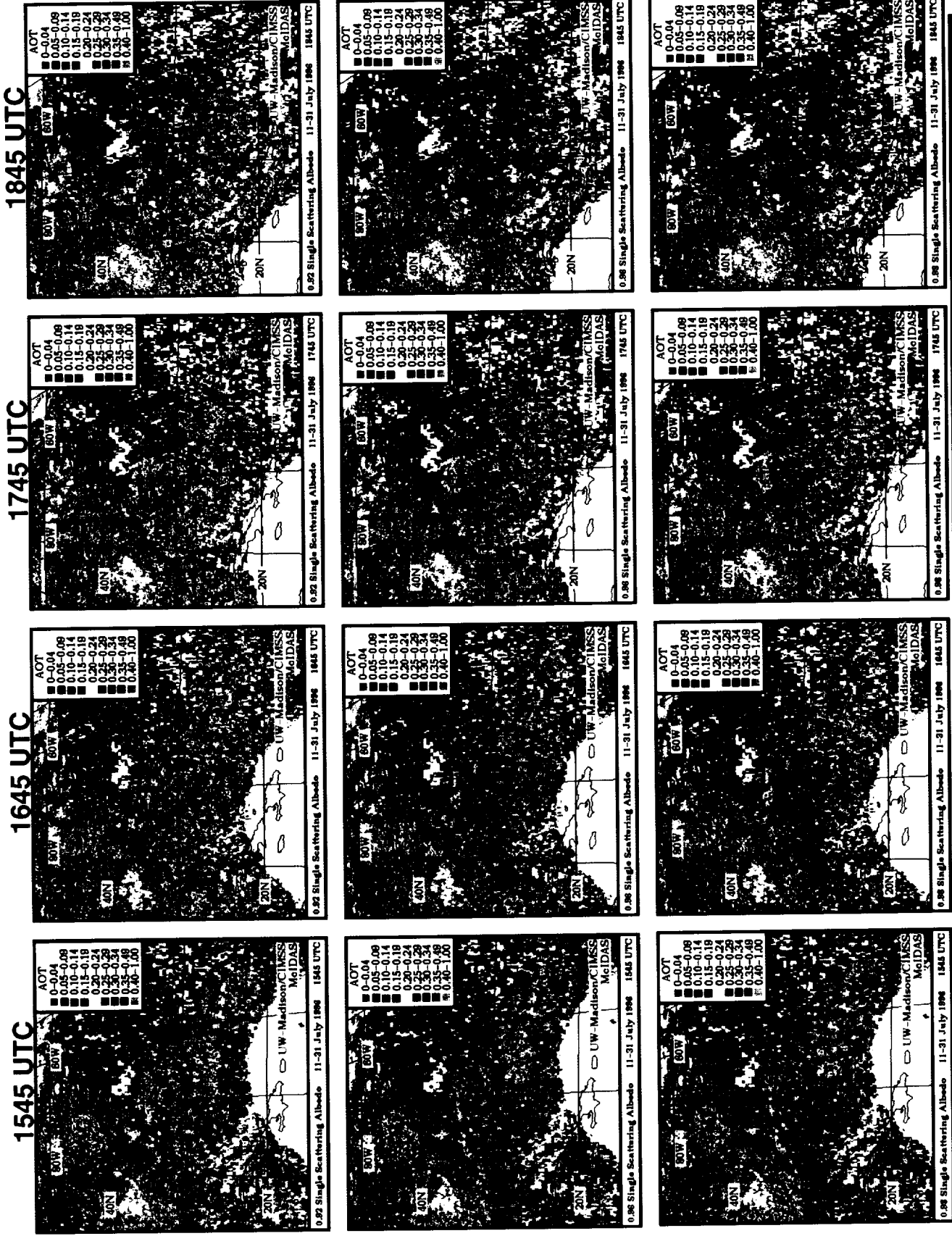
Comparison of GOES-8 Derived AOT Using Single Scattering Albedos of .92, .96, and .98

Date: 21-Jul-96 at 1145, 1245, 1345, 1445 UTC
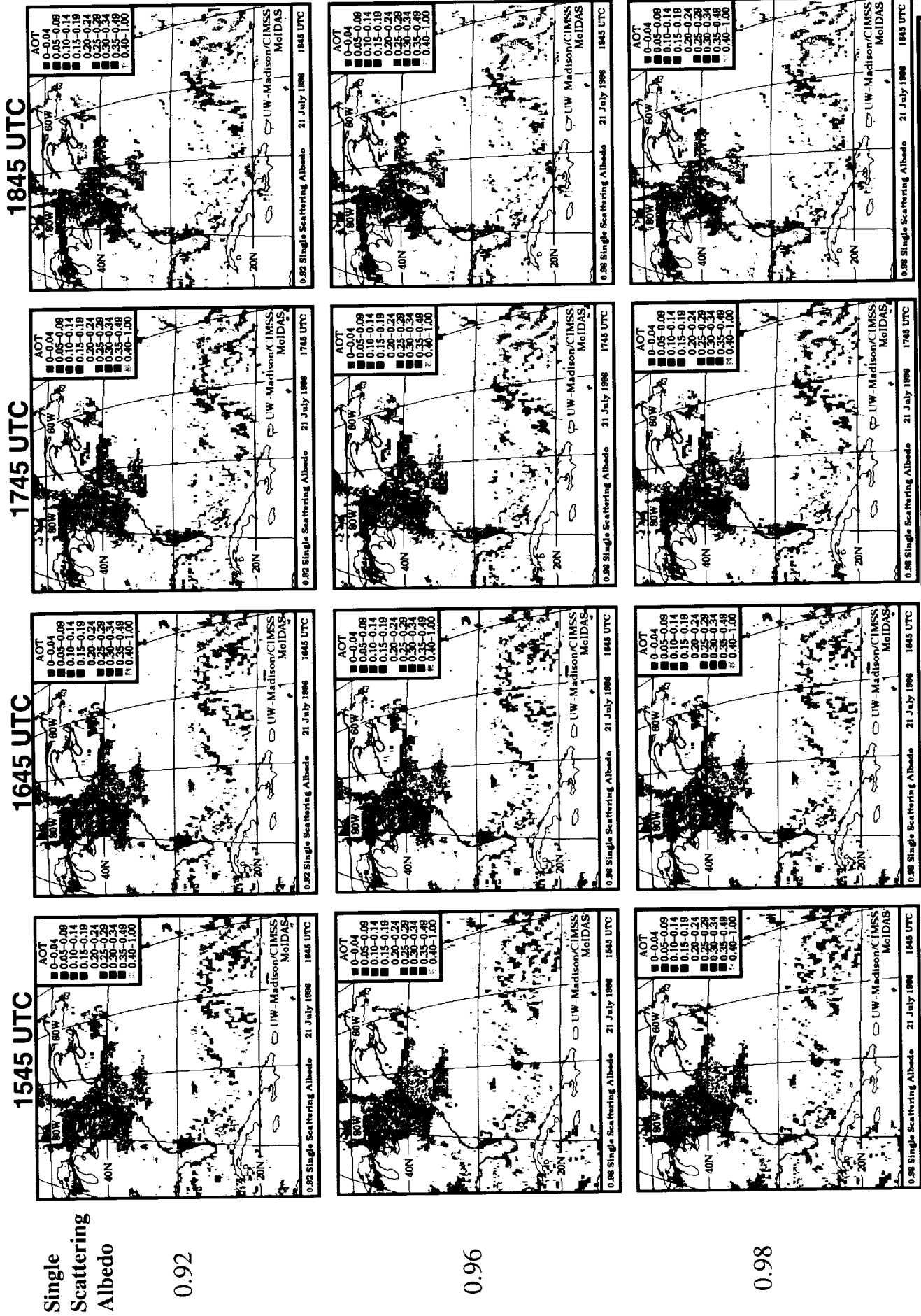
Figure 11

Comparison of GOES-8 Derived AOT Using Single Scattering Albedos of .92, .96, and .98
Date: 21-Jul-96 at 1545, 1645, 1745, 1845 UTC
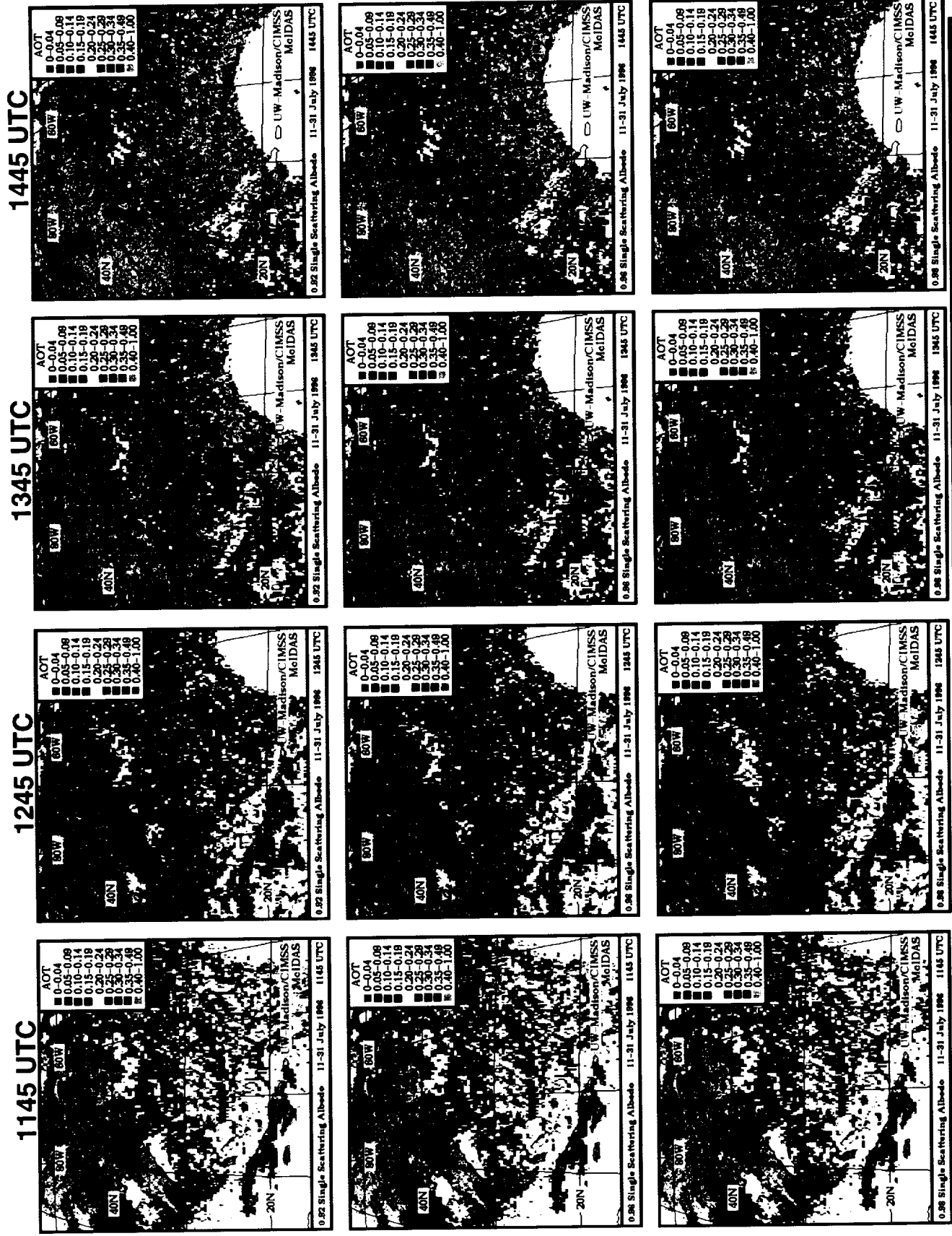
Figure 12

Comparison of GOES-8 Derived AOT Using Single Scattering Albedos of .92, .96, and .98
Date: 11-31 Jul-96 at 1145, 1245, 1345, 1445 UTC

-21-

Figure 13

Comparison of GOES-8 Derived AOT Using Single Scattering Albedos of .92, .96, and .98
Date: 11-31 Jul-96 at 1545, 1645, 1745, 1845 UTC

-22-

Figure 14

GOES-8 Derived AOTs Compared with Sun Photometer Derived AOTs During TARFOX Using Single Scattering Albedos of 0.96, and 0.98
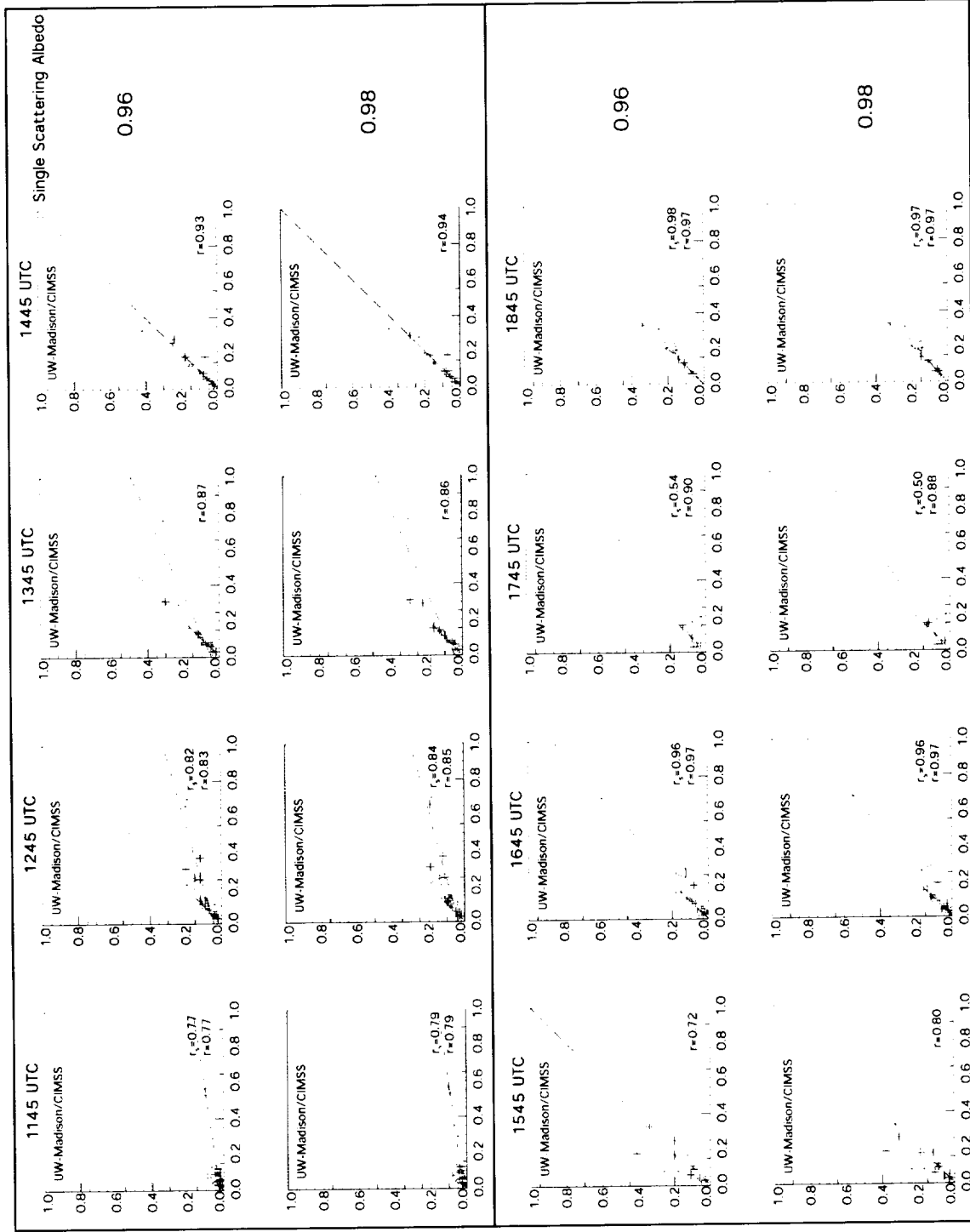
GOES-8 Derived AOT at 0.65 microns

AERONET Sun Photometer AOT at 0.67 microns

Figure 15

when the ship data are included, correlations (r_s) range from 0.50–0.97. Excluding the 1745 UTC case, the ratios of the ship sun photometer derived AOT to the GOES-8 derived AOT are similar to the ratios over land, thus showing good consistency in GOES-8 AOT algorithm performance for both land and water AOT retrieval.

D. A Comparison with the Revised Stowe GOES AOT Algorithm

The new experimental CIMSS GOES-8 AOT was developed to better characterize AOT on land and water by accounting for clear-sky background conditions and applying a more stringent cloud-clearing scheme. Figure 16 provides an example of the difference between the new CIMSS GOES-8 AOT and the revised Stowe GOES-8 AOT at 1845 UTC on 21 July 1996. The revised Stowe example includes an adjustment for sensor degradation and a reduction in resolution to 4 km. The CIMSS algorithm provides some indication of AOT values over land where the revised Stowe algorithm saturated because it was based on direct reflectance rather than a difference above background. For that same reason, the overall AOT values over water are much higher for the revised Stowe algorithm than for the CIMSS GOES-8 AOT. On average the STOWE minus CIMSS AOT difference is approximately 0.30. An examination of figure 16d in combination with the visible image (figure 16a) and the infrared window band (figure 16b) shows how the revised Stowe algorithm retrieves many AOT values that are biased by cloud cover. On the other hand, due to aggressive cloud clearing and the coarse resolution of the cloud-processing scheme, the CIMSS algorithm (figure 16c) has the potential to miss retrievals in regions which are not cloud covered, but are labeled as such because they are adjacent to a cloudy region. Overall, the two algorithms show fairly similar patterns of more optically thick versus thin regions over the ocean.

E. GOES-8 Derived AOTs for Saharan Dust Transport on 11 July 1996

Figure 17 a-c shows streamline analyses on 11 July 1996 at 12 UTC at three levels in the atmosphere. The 850 mb (figure 17a) streamlines show low-level flow south of Bermuda originating off the European and African coasts. North of Bermuda, the low-level flow is originating off the eastern coast of the United States. At the 700 mb (figure 17b) and 500 mb (figure 17c) levels the streamlines indicate the circulation near Bermuda is closed with the dominant flow coming from the African coast.

Figure 17e provides a close-up view of the 700 mb streamlines outlined by the red box in figure 17b. The AOT analysis is for one day later on 12 July 1996 at 1745 UTC. On 12 July 1996, Smirnov et al. (2000) reported AOT observations of Saharan dust near Bermuda. The ship "Meridian" was located at 32.63°N and 64.72°W on 12 July 1996. The approximate location of the ship is shown on figure 17d,e. The ship is within a region of haze apparent on the GOES-8 visible image (figure 17d). AOTs corresponding to this location were 0.20-0.34, within the range of values derived from the ship sun photometer. In addition, the upper level circulation encloses the region of high AOT. Whether the increase in AOT is due to Saharan dust or east coast pollution, is difficult to discern without knowing the physical level of the haze. However, the fact that it is well aligned with the upper level circulation seems to support the possibility that the source is Saharan dust.
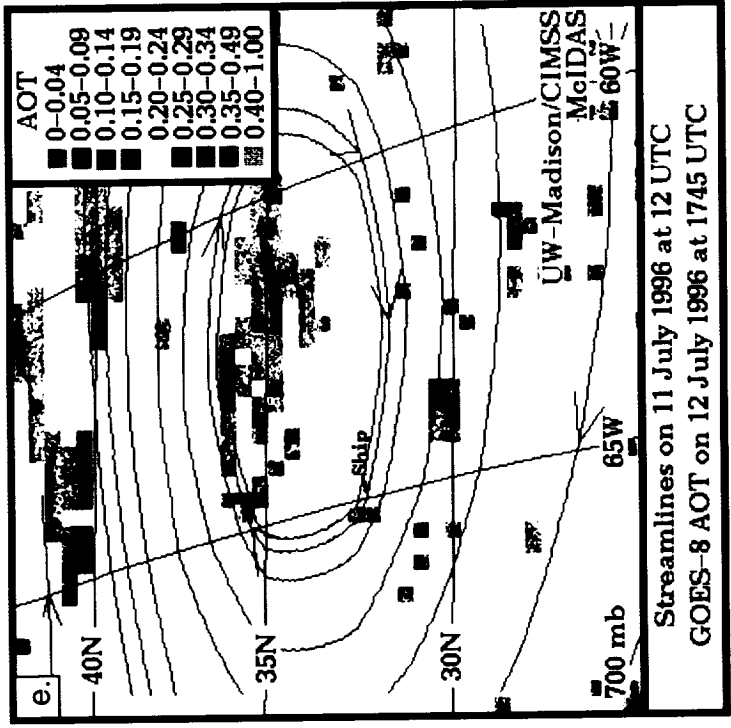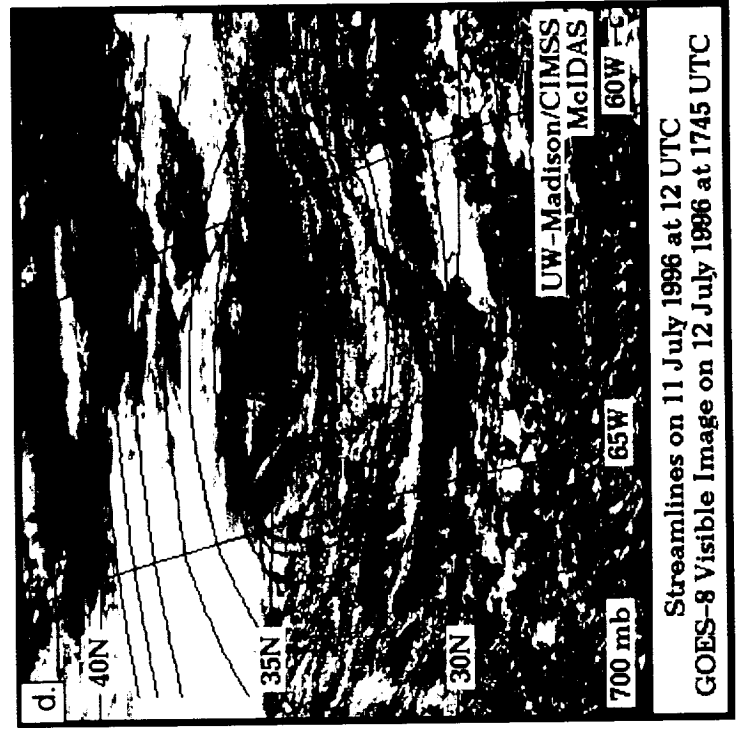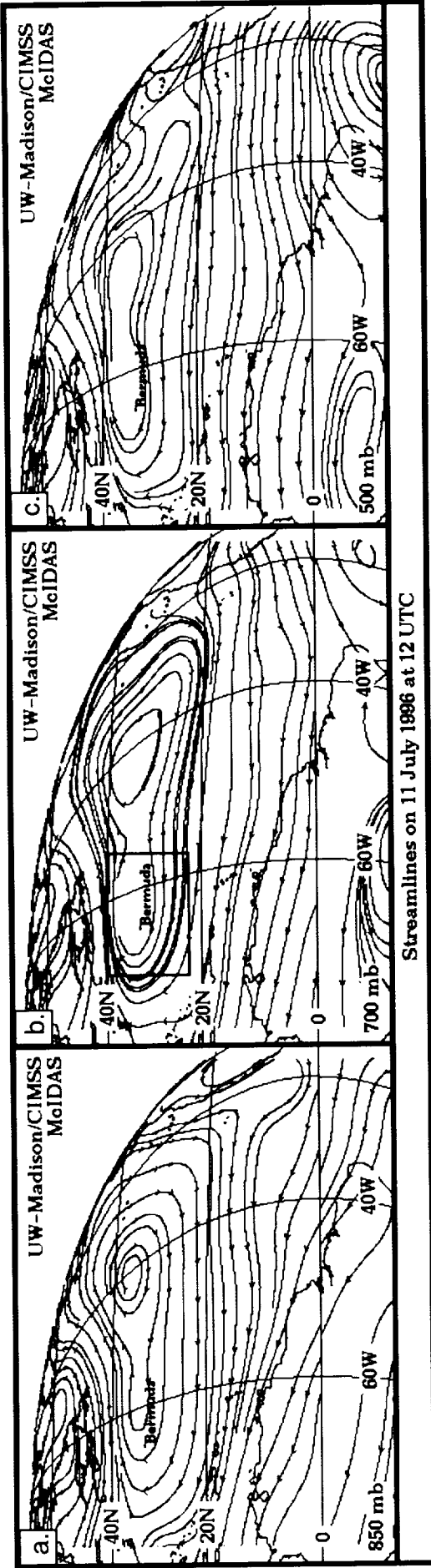
A Comparison of the 0.98 Single Scattering Albedo AOT results
with the Stowe AOT Algorithm for 21-July 1996 at 1845 UTC
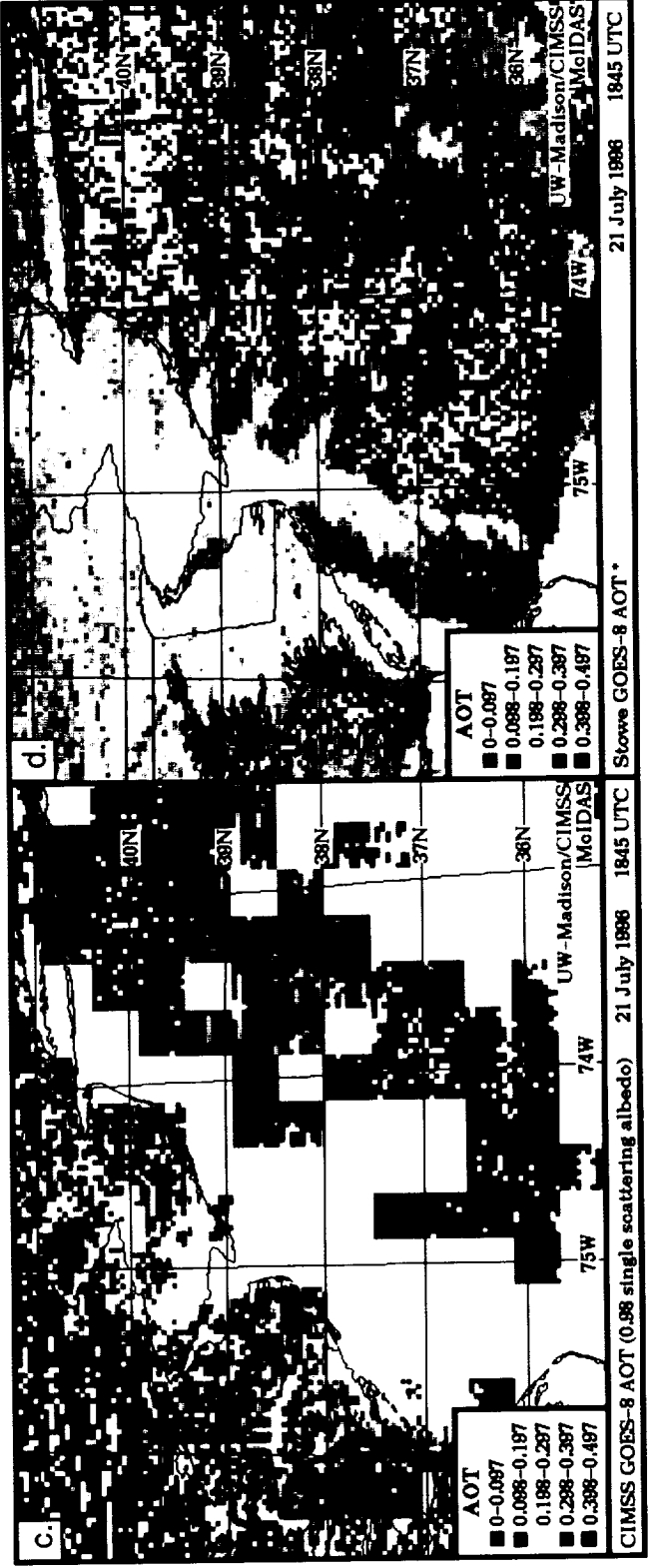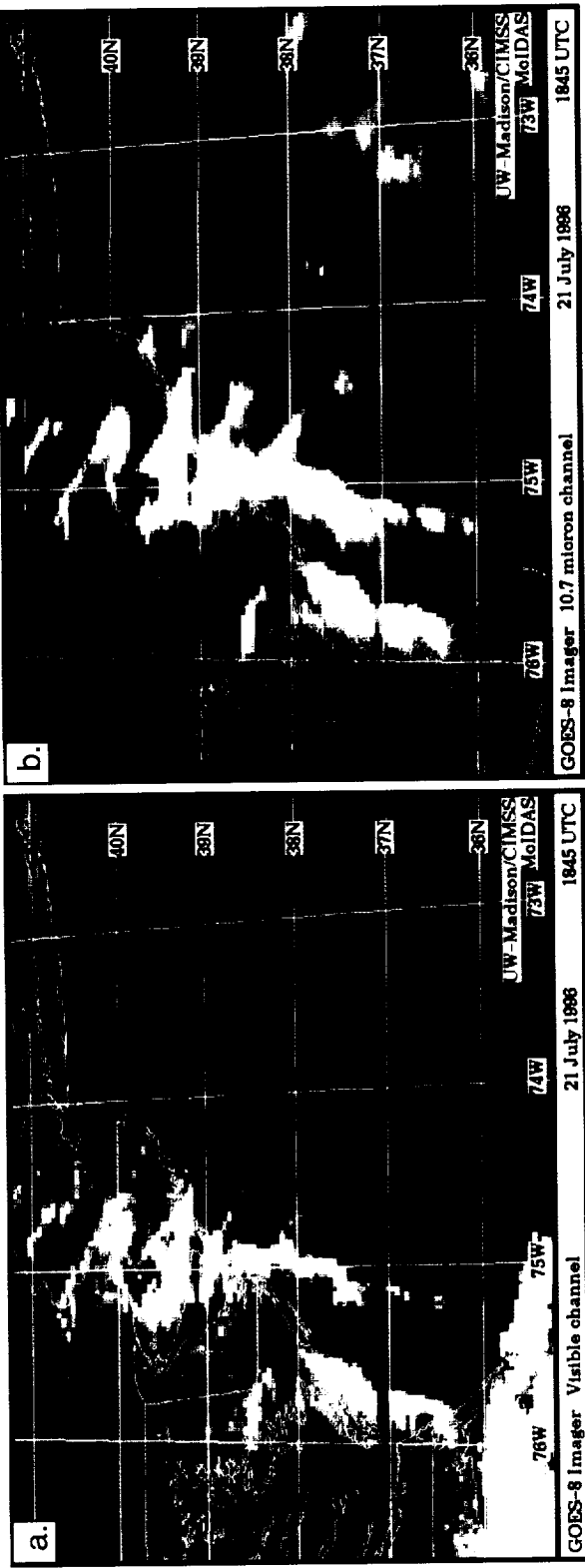
Figure 16

-25-

Observation of Aerosol Layer on 12 July 1996

Figure 17

VII. Future Plans

Although this 3-year effort provided a good overview of the capabilities of geostationary satellites for quantitative measurements of aerosol loading, more work is needed to refine the GOES-8 MACADA and CIMSS GOES-8 AOT. Possible activities are listed below.

- Train the MACADA over North America and study ways of reducing the necessary size of the statistical box. Modifications of the MACADA would enable better discrimination of clear versus cloudy sky observations, especially along cloud edges, at an increased resolution.

- While the ecosystem albedo map was an effective and efficient way to determine background conditions in regions of persistent smoke/cloud coverage, better results may be obtained if background information is filled in from neighboring pixels or similar ecosystems which have comparable viewing geometry.

- Adjust the sensor degradation to reflect the most recent Knapp and Vonder Haar results, examine the impact, and then study a way to reduce the early morning AOT biases caused by viewing geometry.

VIII. Presentations/Publications:

Prins, E.M., J. M. Feltz, R. A. Frey, C. C. Schmidt, W. P. Menzel, D. Wylie, 2000: A five-year trend analysis of biomass burning in South America Using GOES, American Geophysical Union Spring Meeting, May 30 – June 2, 2000, Washington D.C.

Prins, E.M., J. M. Feltz, R. A. Frey, C. C. Schmidt, W. P. Menzel, K. Goodstein, 2001: A Six Year Climatology of Biomass Burning in South America Using GOES, To be submitted.

IX. References:

Knapp, K.R., and T.H. Vonder Haar, 2000: Calibration of the eighth Geostationary Observational Environmental Satellite (GOES-8) imager visible sensor, J. Atmos and Ocean. Tech., 17, 1639-1644.

Smirnov, A., B.N. Holben, O. Dubovik, N.T. O'Neill, L.A. Remer, T.F. Eck, I. Slutsker, D. Savoie, 2000: Measurements of atmospheric optical parameters on U.S. Atlantic coast sites, ships, and Bermuda during TARFOX, J. Geophys. Res., 105, 9887-9901.